

1 **Review article: Terrestrial dissolved organic carbon in northern permafrost**

2 Liam Heffernan¹, Dolly N. Kothawala¹, Lars J. Tranvik¹

3

4 ¹Limnology/Department of Ecology and Genetics, Uppsala University, Norbyvägen 18D,
5 Uppsala 75236, Sweden

6

7 Correspondence email: liam.heffernan@ebe.uu.se, liam.heffernan@vu.nl

Field Code Changed

8

9

10

11

12

13

14

15

16

17

18

19

20

21

22 Abstract

23 As the permafrost region warms and permafrost soils thaw, vast stores of soil organic
24 carbon (C) become vulnerable to enhanced microbial decomposition and lateral transport into
25 aquatic ecosystems as dissolved organic carbon (DOC). The mobilization of permafrost soil C
26 can drastically alter the net northern permafrost C budget. DOC entering aquatic ecosystems
27 becomes biological available for degradation as well as other types of aquatic processing.
28 However, it currently remains unclear which landscape characteristics are most relevant to
29 consider in terms of predicting DOC concentrations entering aquatic systems from permafrost
30 regions. Here, we conducted a systematic review of 111 studies relating to, or including,
31 concentrations of DOC in terrestrial permafrost ecosystems in the northern circumpolar region
32 published between 2000 – 2022. We present a new permafrost DOC dataset consisting of 2,276
33 DOC concentrations, collected from the top 3 m in permafrost soils across the northern
34 circumpolar region. Concentrations of DOC ranged from 0.1 – 500 mg L⁻¹ (median = 41 mg L⁻¹)
35 across all permafrost zones, ecoregions, soil types, and thermal horizons. Across permafrost
36 zones the highest median DOC concentrations were ~~greatest~~ in the sporadic permafrost zone
37 (101 mg L⁻¹) while lower concentrations were found in the discontinuous (60 mg L⁻¹) and
38 continuous (59 mg L⁻¹) permafrost zones. However, median DOC concentrations varied in these
39 zones across ecosystem type, with ~~the~~ the highest median DOC concentrations in each
40 ecosystem type of 66 mg L⁻¹ and 63 mg L⁻¹ ~~were~~ found in coastal tundra and permafrost bog
41 ecosystems, respectively. Coastal tundra (130 mg L⁻¹), permafrost bogs (78 mg L⁻¹), and
42 permafrost wetlands (57 mg L⁻¹) had the highest median DOC concentrations in the permafrost
43 lens, representing a potentially long-term store of DOC. Other than in Yedoma ecosystems, DOC
44 concentrations were found to increase following permafrost thaw and were highly constrained by
45 total dissolved nitrogen concentrations. This systematic review highlights how DOC
46 concentrations differ between organic- or mineral-rich deposits across the circumpolar
47 permafrost region and identifies coastal tundra regions as areas of potentially important DOC
48 mobilization. The quantity of permafrost-derived DOC exported laterally to aquatic ecosystems
49 is an important step for predicting its vulnerability to decomposition.

50

51 **1. Introduction**

52 Persistent freezing temperatures since the late Pleistocene and Holocene has led to the
53 accumulation and preservation of 1,460 – 1,600 Pg of organic carbon (C) in northern
54 circumpolar permafrost soils (Hugelius et al., 2014; Schuur et al., 2018). However, in recent
55 decades, there has been an amplified level of warming at high latitudes, occurring at four-times
56 the speed of the global average (Rantanen et al., 2021). This is leading to widespread and rapid
57 permafrost thawing which is predicted to continue under various future climate scenarios
58 (Olefeldt et al., 2016). Under the high C emissions representative concentration pathway
59 (RCP8.5), 90% loss of near-surface permafrost is projected to occur by 2300, with the majority
60 of loss occurring by 2100 (McGuire et al., 2018). Increasing temperatures and widespread thaw
61 exposes permafrost C to heterotrophic decomposition, potentially leading to enhanced emissions
62 of greenhouse gases to the atmosphere in the form of carbon dioxide (CO₂; Schuur et al., 2021)
63 and methane (CH₄; Turetsky et al., 2020). Additionally, previously frozen soil organic carbon
64 may be mobilized into the aquatic network as dissolved organic carbon (DOC), the quantity and
65 quality of which will likely depend on local and regional hydrology, and landscape
66 characteristics (Tank et al., 2012; Vonk et al., 2015). At high latitudes (>50°N), lakes and rivers
67 of various sizes cover 5.6% and 0.47% of the total area, respectively (Olefeldt et al., 2021), and
68 the landscape C balance at these high latitudes is highly dependent on aquatic C processing
69 (Vonk & Gustafsson, 2013). The increased leaching of recently thawed DOC from permafrost
70 soils will increase the currently estimated 25 – 36 Tg DOC year⁻¹ exported into the freshwater
71 system, and subsequently into the Arctic Ocean (Holmes et al., 2012; Raymond et al., 2007). It
72 may also lead to enhanced greenhouse gas emissions from freshwater ecosystems (Dean et al.,
73 2020). However, uncertainty remains as to which terrestrial ecosystems contain the highest
74 concentrations of DOC, laterally transport the greatest quantities of DOC, and represent the store
75 of DOC most vulnerable to mineralization.

76 Globally, DOC concentrations have been shown to vary across biomes, and spatial and
77 temporal scales (Guo et al., 2020; Langeveld et al., 2020). It has been suggested that at such
78 macro scales hydrology, climate, vegetation type, and soil type are important drivers of DOC
79 ~~concentrations~~ concentrations (Langeveld et al., 2020). Hydrology and climate are important
80 factors shaping ecosystem structure and function in permafrost regions (Andresen et al., 2020;

81 Wang et al., 2019), which in turn influences the spatial distribution of vegetation and soil types.
82 Vegetation type has been shown to be the most important driver of DOC concentrations in Arctic
83 lakes (Stolpmann et al., 2021). Carbon uptake by vegetation, via gross primary production, and
84 SOC stocks in the permafrost region have both been shown to vary across vegetation and soil
85 types (Ma et al., 2023; Hugelius et al., 2014). This variability across vegetation and soil types
86 has important implications for DOC production, which is associated with plant inputs (Moore &
87 Dalva, 2001) and the decomposition and solubilization of SOC due to soil microbial activity
88 (Guggenberger & Zech, 1993). In permafrost soils, the majority of this production is likely to
89 occur near the soil surface as the microbial production of DOC via input of plant-derived labile
90 substrates has been shown to decrease with depth (Hultman et al., 2015; Monteux et al., 2018;
91 Wild et al., 2016) and 65 – 70 % of the SOC store is found in the top 3 m (Hugelius et al., 2014).
92 The spatial distribution discrepancies observed in DOC concentrations from global assessment
93 efforts (Guo et al., 2020; Langeveld et al., 2020) may be reduced for the circumpolar permafrost
94 region by improving understanding of DOC concentrations in the top 3 m across ecosystem
95 types.

96 Previous studies have highlighted that the mineralization and lateral transport of DOC, i.e.,
97 mobilization, represents a source of terrestrial permafrost C that can potentially play an
98 important role in both terrestrial and aquatic biogeochemical cycles (Hugelius et al., 2020;
99 Parmentier et al., 2017; Schuur et al., 2022). However, none have quantified DOC mobilization
100 across the permafrost region. Inclusion of DOC mobilization in attempts to determine the
101 permafrost climate feedback (Schaefer et al., 2014), may reduce current uncertainty in the
102 magnitude and location of permafrost C losses (Miner et al., 2022), particularly as permafrost
103 thaws. Warming of near surface permafrost causes widespread thawing (Camill, 2005; Jorgenson
104 et al., 2006), which can lead to drastic changes in hydrology, vegetation, and soil carbon
105 dynamics (Liljedahl et al., 2016; Pries et al., 2012; Varner et al., 2022), thus impacting both
106 DOC production and mobilization. Several studies have demonstrated that DOC has the potential
107 to be rapidly degraded and mineralized following thermokarst formation (Burd et al., 2020;
108 Payandi-Rolland et al., 2020; Wickland et al., 2018), particularly in higher latitude ecosystems
109 (Ernakovich et al., 2017; Vonk et al., 2013). However, few have compared this lability across
110 ecosystems (Abbot et al., 2014; Fouche et al., 2020; Textor et al., 2019) and less have done so

111 across the permafrost region (Vonk et al., 2015). Determining the ecosystems with the greatest
112 store of DOC that is readily mineralized upon thermokarst formation represents a potentially
113 important step in reducing uncertainty in the permafrost climate feedback.

114 Here, we conduct a systematic review of the literature and compiled 111 studies published
115 between 2000 – 2022 on DOC concentrations in the top 3 m of soil in terrestrial ecosystems
116 found in the northern circumpolar permafrost region. Our aim was to build a database to assess
117 the concentration and mobilization of DOC across terrestrial permafrost ecosystems. We used
118 this database to address the following hypotheses; (i) the highest DOC concentrations would be
119 found in organic rich wetland ecosystems; (ii) disturbance would lead to increased export and
120 biodegradability of DOC; and (iii) the most biodegradable DOC would be found in Yedoma and
121 tundra ecosystems. A quantitative assessment of studies pertaining to DOC concentrations in
122 permafrost soils can identify evidence-based recommendations for future topics, standardisation
123 of methods, and areas of research to improve our understanding on terrestrial and aquatic
124 biogeochemical cycling in northern permafrost regions. Our database contains ancillary data
125 describing the geographical and ecological conditions associated with each DOC concentration,
126 allowing us to reveal patterns in DOC concentrations and lability measures for 562 sampling
127 sites across multiple ecosystem types and under varying disturbance regimes. This study
128 represents the first systematic review of DOC concentrations within terrestrial permafrost
129 ecosystems found in the circumpolar north. As such, it provides unique and valuable insights into
130 identifying ecosystems associated with the highest DOC concentrations, and thus ecosystems
131 with the greatest potential for DOC mobilization.

132 **2. Methods**

133 This systematic review used a methodological framework proposed by Arksey &
134 O'Malley (2005) and follows five steps: 1) develop research questions and a search query; 2)
135 identify relevant studies; 3) study selection; 4) data extraction; and 5) data analysis, summary,
136 and reporting. The literature search was guided by four research questions: 1) what are the
137 concentrations of DOC found in terrestrial ecosystems across the northern circumpolar
138 permafrost region?; 2) what are the rates of export and/or degradation (mobilization) of DOC
139 within these ecosystems?; 3) What are the major controls on DOC concentrations and rates of
140 mobilization?; and 4) how are concentrations and mobilization rates impacted by thermokarst

141 formation? Mobilization rates represent DOC loss and include specific discharge of DOC (g
142 DOC m⁻²), export rate of DOC per day (g C m⁻² day⁻¹) and per year (g C m⁻² year⁻¹), and
143 biodegradable DOC (BDOC; %).

144 2.1 Literature Search

145 Based on *a priori* tests, we used the following search query string to find papers using
146 information found in their title, abstract, and keywords: ("dissolved organic carbon") AND
147 (permafrost OR thermokarst OR "thaw slump") AND (soil OR peat) AND (export OR degrad*
148 OR decomposition OR mineralization). We used Web of Science, Science Direct, Scopus,
149 PubMed, and Google Scholar to generate a database of tier 1, peer-reviewed articles published
150 between 2000 – 2022. The search function on Science Direct does not support the use of
151 wildcards such as "*", so "degrad*" was changed to "degradation". We removed duplicate
152 references found across multiple databases using Mendeley© referencing software (v1.17.1,
153 Mendeley Ltd. 2016). ~~We used the same search query string as above to search for articles on the
154 first 15 pages of Google Scholar. This resulted in the addition of a further 150 articles to be
155 included in our systematic screening process.~~

156 2.2 Systematic Screening of Peer-Reviewed Publications

157 The selection of relevant studies was comprised of inclusion criteria and relevance
158 screening in three steps. In the first step we placed limits on initial study searches in the
159 electronic databases mentioned above. Studies were included in the review if they were primary
160 research, published in English, and published between 2000 – 2022 (Table 1). Only quantitative
161 studies conducted in terrestrial ecosystems within the northern circumpolar permafrost region, as
162 defined by Brown et al., (1997), and reporting DOC concentration and mobilization rates were
163 included. Studies not meeting these criteria were eliminated and the remaining studies proceeded
164 to the second screening step.

Table 1. Summary of criteria used to identify suitable studies in the preliminary screening stage

	Inclusion criteria	Exclusion criteria
Timeline	Study published between 2000 – 2022	Study published prior to 2000

Study type	Primary research article published in peer-reviewed journal using quantitative methods	Thesis/dissertations and secondary research studies (reviews, commentaries, editorials)
Language	Published in English	Studies published in other languages
Region	Conducted within the northern circumpolar permafrost region	Conducted outside of the northern circumpolar permafrost region
Outcome	Studies on DOC concentration, export or degradation in permafrost environments	Studies not on DOC concentration, export or degradation in permafrost environments

165

166 In the second step, the primary relevance of articles was screened, based on article titles,
167 abstracts, and keywords, and the eligibility criteria provided in Table 2. Studies deemed
168 irrelevant were eliminated and the remaining studies proceeded to the third and final screening
169 step, or secondary screening stage, which was based on was based on more specific eligibility
170 criteria (Table 2) applied to the full text.

Table 2. Primary and secondary relevance screening tools. Primary screening tool used in the article title, abstract, and keyword screening stage. Secondary screening tool used in full-text screening stage

Screening stage	Screening questions	Response details
Primary	Does the study involve quantitative data collected from a permafrost environment?	Yes – reports on quantitative data collected from a permafrost environment No – does not report on the above
Primary and Secondary	Is the study region within the northern circumpolar permafrost region?	Yes – reports on quantitative data (including field observations and lab data) collected from the circumpolar permafrost environment. No – study region is not in the northern circumpolar permafrost regions; other examples could be mountainous permafrost or Tibetan plateau
Primary and Secondary	Is the article in English and NOT a review, book chapter, commentary, correspondence,	Yes – study is in English and is a primary research article that includes quantitative studies (field and lab based), including model-based research as it relies on observational data.*

	letter, editorial, case report, or reflection?	No – study is not in English and/or is a review, book, editorial, working paper, commentary, conference proceeding, supplementary text, or qualitative study which does not address outcomes relevant to this review
Primary and Secondary	Does the study involve the concentration, export or degradation of terrestrially derived DOC?	Yes – reports on terrestrial DOC concentration, export, or degradation, including concentrations and characterization No – does not report on terrestrial DOC concentration, export, or degradation
Secondary	Is the article in English, longer than 500 words, and published between 2000 - 2022?	Yes – study is published between 2000 – 2022 No – study is published prior to 2000

171 *For model-based studies, the original field/lab data used to parametrise or develop the model
172 was used. If this data was taken from previously published work, then those studies were used
173 and the model-based study removed.

174 *2.3 Database compilation*

175 A database with reported DOC concentrations and mobilization rates i.e., rates of either
176 DOC export or degradation, was compiled using data from all studies that were deemed relevant
177 following the study selection phase. The database was compiled to compare DOC concentrations
178 and mobilization rates between different sites. We define a site as an area where either soil,
179 water, or ice samples were taken from that has similar vegetation composition, water table
180 position, permafrost regime, and was either disturbed or pristine. Site descriptions were derived
181 from the text of each study. Where possible, individual daily measurements of DOC
182 concentrations and mobilization rates were taken. When replicates of the same daily
183 measurement were provided, we used the mean of those replicates, which was relevant for 10
184 studies within the database, representing 72 DOC concentrations. All data was extracted from
185 data tables, text, supplementary material, or extracted from data figures using WebPlotDigitizer
186 (<https://automeris.io/WebPlotDigitizer>).

187 All studies reported measuring DOC concentrations collected from either open-water, pore
188 water, ice, or soil using a median filter pore size of 0.45 µm with first and third quartiles pore
189 size of 0.45 and 0.7 µm. Measurements from all 12 months of the year were included in the

190 database with the majority occurring during the growing season (May – August), a small portion
191 during the non-growing season, and the remaining sampling times were either not reported or are
192 averages over multiple sampling occasions. We included data from studies that were both field
193 and lab based. However, any data where a treatment was applied was excluded, except for
194 temperature treatments during incubation experiments when assessing the biodegradability of
195 DOC. When lab-based studies included an incubation, only Day 0 DOC concentrations were
196 used when comparing DOC concentrations across studies. We chose to remove any DOC
197 concentrations from samples taken below 3 m depth, which represented 3% of all DOC
198 measurements. These measurements were removed for better comparability with the current best
199 estimation of soil organic carbon stocks within the northern circumpolar permafrost zone
200 (Hugelius et al., 2014). We also removed any DOC concentrations greater than 500 mg L⁻¹,
201 which represented 2% of all DOC concentrations. Samples that were above 500 mg L⁻¹ and were
202 sampled below 3 m represented 1% of all DOC concentrations.

203 Site averaged daily DOC concentrations (mg L⁻¹) and mobilization rates were estimated from
204 the average concentration and mobilization rates measured within a single day or sampling
205 occasion. Repeated measurements at a site, either over the growing season or multiyear
206 measurements, were treated as an individual estimate of DOC concentrations and mobilization
207 rates. Other continuous variables that were similarly estimated include soil moisture, water table
208 position, organic layer depth, active layer depth, bulk density of soil, soil carbon content (%),
209 soil nitrogen content (%), soil carbon:nitrogen (C:N), pH, electrical conductivity (μS cm⁻¹),
210 specific UV absorbance at 254 nm (SUVA; L mg C⁻¹ m⁻¹), total dissolved nitrogen (mg L⁻¹),
211 nitrate (mg L⁻¹), ammonium (mg L⁻¹), chloride (mg L⁻¹), calcium (mg L⁻¹), and magnesium (mg
212 L⁻¹). The aromatic content of organic matter is positively correlated with SUVA (Weishaar et al.,
213 2003), with high SUVA values being used as an indication of high aromatic content (Hansen et
214 al., 2016). Ratios of soil C:N have been shown to be a good proxy for decomposition (Biester et
215 al., 2014), where high C:N values indicate higher decomposition has previously occurred. Mean
216 annual temperatures and precipitation, sampling depth, filter size, the number of days over which
217 sampling took place, how many years following disturbance measurements were taken were also
218 recorded. Several continuous variables other than those mentioned above were also recorded in
219 the database, but not used for analysis if they represented < 20% of the database. We chose 20%

220 as the cut-off point for use in comparison of the relationship between DOC concentrations and
221 mobilization with other site continuous variables.

222 Categorical variables included in the database [\(Table S1\)](#) were site location within the
223 permafrost zone (continuous, discontinuous, sporadic; Brown et al., 1997) and ecoregion (arctic
224 tundra, sub-arctic tundra, sub-arctic boreal, and continental boreal; Olson et al., 2001). We
225 included site surface permafrost conditions (present or absent), the thermal horizon layer
226 sampled (active layer, permafrost [lens](#), permafrost free, water, and thaw stream), and if present
227 what type of disturbance occurred at the site (fire, active layer thickening, thermokarst terrestrial,
228 or thermokarst aquatic). Active layer represents the seasonally unfrozen soil layer above the
229 permafrost layer. Permafrost [lens](#) represents the permanently frozen (below 0 °C) layer.
230 Permafrost lens DOC concentrations are determined from soil and pore water within the
231 permafrost layer and extracted via frozen cores, whereas active layer samples are taken from soil
232 cores or porewater that are unfrozen at the time of sampling. Thaw Stream represents flowing
233 surface waters following permafrost thaw. Permafrost Free represents areas that are not underlain
234 by permafrost. We also included the soil class found at the site (Histel, Histosol, Orthel, and
235 Turbel; USDA, 1999) and whether the DOC was from the organic or mineral soil. Histosols are
236 organic rich, non-permafrost soils. Histels, Orthels, and Turbels are permafrost-affected soils
237 (Gelisol order). Histels are organic rich, Orthels are non cryoturbated affected mineral soils, and
238 Turbels are cryoturbated permafrost soils. Organic rich Histel and Histosol soils have been
239 previously shown to contain greater SOC stocks in the top 3 m of soil than the mineral rich
240 Orthel and Histel soils (Hugelius et al., 2014). To assess the influence of sampling approach and
241 method of analysis, we included method of DOC extraction (centrifugation of soil sample,
242 leaching and dry leaching of soil, dialysis, grab sample, ice core extraction, potassium sulphate
243 extraction, lysimeter, piezometer, pump, rhizons) and DOC measurement method (combustion,
244 persulphate, photometric, or solid-phase extraction).

245 Sites were classified according to ecosystem type, and these included coastal tundra, forest,
246 peatland, permafrost bog, permafrost wetland, retrogressive thaw slump, upland tundra, and
247 Yedoma. Ecosystem classification is based on the general site description in the article, the
248 provided ecosystem classification within the article, and site data including vegetation
249 composition, permafrost conditions, and ecoregion. Coastal tundra sites includes typical

250 polygonal tundra features found along the coastline in the permafrost region (Lantuit et al.,
251 2012). Forests include any forested ecosystem, such as a black spruce forest (Kane et al., 2006)
252 or larch forest (Kawahigashi et al., 2011) where the soil is not a wetland soil. Peatlands are sites
253 classified as either fens (Olefeldt and Roulet 2012) or bogs (Olsrund and Christensen 2011) that
254 are within the permafrost domain but are not underlain by permafrost. Permafrost bogs are sites
255 that are bogs and are either underlain by permafrost (O'Donnel et al., 2016) or are thermokarst
256 bogs (Burd et al., 2020) that were previously underlain by permafrost prior to thawing.
257 Permafrost wetlands sites include saturated soils that are underlain by permafrost, or were
258 previously underlain by permafrost prior to permafrost thaw. They contain sampling locations
259 typical of moist acidic tundra (Trusiak et al., 2018), tundra meadows (Tanski et al., 2017), and
260 high-latitude fens (Nielsen et al., 2017). Retrogressive thaw slumps are areas where substantial
261 ground ice degradation leads to thermokarst and the resulting feature contains a retreating
262 headwall (Abbott et al., 2015). Upland tundra sites are high-latitude, non-wetland, mineral soils
263 that include tundra heath (Stutter and Billett 2003) and meadows (Hirst et al., 2022). Yedoma
264 sites include pristine forest, upland tundra, and coastal tundra, as well as retrogressive thaw
265 slumps and other thermokarst features found within the Yedoma permafrost domain (Strauss et
266 al., 2021). The ecosystem classification retrogressive thaw slump only includes these
267 thermokarst features found outside the Yedoma permafrost domain. Each ecosystem type was
268 further classified based on the type of permafrost thaw or thermokarst formation that occurred
269 there. These thaw or thermokarst types included thermokarst bog, thermokarst wetland, active
270 layer thickening, retrogressive thaw slump, exposure, thermo-erosion gully, and active layer
271 detachment.

272 *2.4 Database analysis*

273 All statistical analyses were carried out in R (Version 3.4.4, R Core Team, 2015). We aimed
274 to assess how DOC concentrations differed across study regions and ecosystems. To do this we
275 used Kruskal-Wallis analysis to test for differences in median DOC concentrations among the
276 various study regions and areas that included permafrost zones, ecoregions, soil class, thermal
277 horizon, and ecosystems. Post-hoc comparisons of median DOC concentrations among these
278 categories were performed using pairwise Wilcox test. Within and between each ecosystem type
279 we assessed the differences in DOC concentrations found in different thermal horizons (i.e.,

280 active layer and permafrost lens). To do this, data was first transformed using a Box Cox
281 transformation and the optimal λ using the *MASS* package (Ripley et al., 2019). We then
282 performed analysis of covariance (ANCOVA) to test for differences in DOC concentrations in
283 different thermal horizons between ecosystem types, while controlling for seasonal effects by
284 including the month in which sampling occurred as the covariate.

285 Following the assessment of differences in DOC concentrations across these study regions
286 and ecosystems we aimed to assess the influence of extraction and analysis method on DOC
287 concentrations. The aim of this was to determine if extraction and analysis method was having a
288 greater effect on DOC concentrations than study region or ecosystem. To do so we first used
289 ANOVAs and Bonferroni post-hoc tests on linear mixed effects models, that include either
290 extraction method, filter size, or analysis method as a fixed effect and ecosystem type as a
291 random factor, to evaluate significant differences in DOC concentrations between DOC
292 extraction and measurement methods. We then performed Kruskal-Wallis analysis to test for
293 differences in median DOC concentrations among the extraction method, filter size, and analysis
294 method in each permafrost zone, ecoregion, soil class, thermal horizon, and ecosystem. Post-hoc
295 comparisons of median DOC concentrations among these categories were performed using
296 pairwise Wilcox test.

297 We used partial least squares regression (PLS) when assessing the relationship of DOC
298 concentrations with continuous and categorical variables. We performed this analysis to
299 determine how the drivers of DOC concentrations across ecosystems may explain the variability
300 in DOC concentrations. Predictor variables were categorized based on their Variable Importance
301 in Projections (VIP) method in the *plsVarSel* package (Mehmood et al., 2012), whereby variables
302 with a score $> 0.6 - 1$ are deemed to be significant (Chong and Jun 2005). We ran several PLS
303 including predictor variables with a VIP of $> 0.6, 0.7, 0.8, 0.9,$ and 1 . The most parsimonious
304 PLS model contained predictor variables with a $VIP > 1$ and was selected based on the
305 proportion of variability in the predictors explained by the model, significant PLS components,
306 Q^2 , and background correlation (Andersen and Bro 2010). PLS was performed using the *pls*
307 package (Mevik & Wehrens, 2007) and we chose to use PLS as it is tolerant of co-correlation of
308 predictor variable, deviations from normality, and missing values, all of which were found within
309 the database. In the PLS ecosystem classes were subdivided into pristine or disturbed (i.e.,

310 impacted by permafrost thaw). Pristine sites were further subdivided by the thermal horizon in
311 which the DOC concentrations were measured (active layer and permafrost lens). Sites were split
312 into disturbed and pristine to assess whether disturbances has an impact on DOC concentrations.
313 Pristine sites were divided by their thermal horizon to assess whether DOC concentrations were
314 more positively related to the active layer exposed to both microbial decomposition and fresh
315 annual carbon inputs from surface vegetation, or the permafrost lens.

316 To evaluate the change in ecosystem DOC concentrations following thermokarst formation,
317 based on all studies from the systematic review, we calculated the response ratio using the
318 *SingleCaseES* package (Pustejovsky et al., 2021). We define thermokarst as the process by which
319 ice-rich permafrost deposits undergo complete thaw, resulting in surface subsidence and the
320 formation of a new, thermokarst feature that is ecological different regarding water table
321 position, redox conditions, and vegetation type, from the preceding pristine ecosystem. Very few
322 studies in our database report DOC concentrations for both pristine and thermokarst affected
323 ecosystem (< 20 %). To include as much data as possible we chose an effect size metric that is
324 unlikely to be influenced by studies with large sample number and variance. The response ratio
325 is;

$$326 \text{ Pristine to Thermokarst Effect Response ratio} = \ln\left(\frac{X_P}{X_T}\right) \quad \text{Eqn. 1}$$

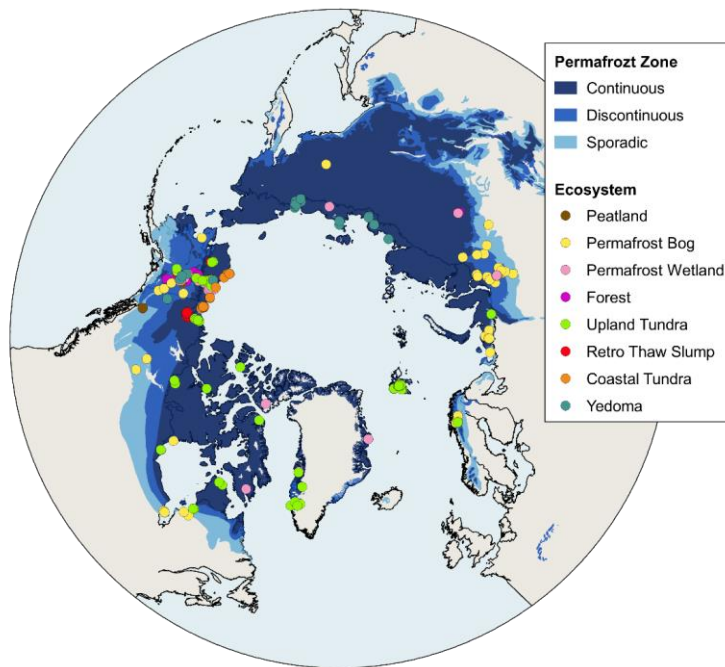
327 where X_P = mean DOC concentration of pristine ecosystems and X_T = mean DOC concentration of
328 thermokarst effected ecosystems (Lajeunesse, 2011). This represents the log proportional
329 difference in mean DOC concentrations between thermokarst and pristine ecosystems, where a
330 positive response ratio indicates a decrease in DOC concentrations following thermokarst.

331 The distribution of the data was inspected visually and with the Shapiro–Wilk test. We tested
332 homogeneity of variances using the *car* package and Levene’s test (Fox and Weisberg, 2011).
333 We report DOC concentrations as the median value with uncertainty as \pm the interquartile range,
334 except for response ratios which we report as \pm 95% confidence intervals. We here define the
335 statistical significance level at 5%.

336 **3. Results**

337 **3.1 Database generation**

338 Our initial search using Web of Knowledge, Science Direct, Scopus, PubMed, and
339 Google Scholar returned a total of 577 unique papers published between 2000 – 2022 that assess
340 the concentrations and rates of mobilization of DOC in terrestrial ecosystems within the northern
341 circumpolar permafrost region. Of these initial 577 studies, 111 remained after the systematic
342 screening process (Table 1 & 2). From these 111 studies we generated our database. The final
343 database of 111 studies contained a total of 3,340 DOC concentrations (mg L^{-1}), with 2,845 DOC
344 concentrations between 0 – 500 mg L^{-1} , found within the top 3 m of permafrost soils from field
345 and lab-based studies (using only Day 0 lab-based DOC concentrations). These concentrations
346 were taken from 562 different sampling locations, representing 8 different ecosystem types
347 (Figure 1; [Table S1](#)+[Table S2](#)) across the northern circumpolar permafrost region. All studies
348 except, for one (Olefeldt et al., 2012), reported DOC concentrations.



349

350 Figure 1. Map of sampling locations where DOC measurements (n=562) from the top 3 m for
351 each ecosystem type. In many cases, the same sampling location was used in multiple studies
352 leading to some overlap, therefore the number of sampling sites included in the data set (562)
353 are not all clearly identifiable from this map. Similarly, several points overlay others even when
354 the ecosystems differ. For a full list of site coordinates please see the database (repository link).
355 Retro Thaw Slump = Retrogressive Thaw Slump. Blue shading represents permafrost zonation
356 (Brown et al., 1997).

357

358 The final database contained a considerably lower number of DOC mobilization
359 measurements. The database includes 16 measurements of specific discharge of DOC (g DOC m^{-2})
360 from 3 studies, 9 export rate of DOC per day ($\text{g C m}^{-2} \text{ day}^{-1}$) and per year ($\text{g C m}^{-2} \text{ year}^{-1}$)
361 measurements were each found in 2 studies. The number of specific discharge, export of DOC
362 per day, and export of DOC per year measurements combined were <1% of the number of DOC
363 concentration measurements. As such they were not considered for analysis of DOC
364 mobilization. A total of 146 BDOC (%) measurements, 4% of the total number of DOC
365 concentration measurements, were found in 14 studies. These measurements of BDOC were
366 from Yedoma (30:5, number of measurements:studies), Upland Tundra (55:5), Forest (18:3),
367 Permafrost Wetland (12:2), and Permafrost Bog (31:5) ecosystems. Given the low number of
368 other forms of DOC mobilization and relatively comparable spread of BDOC measurements
369 across ecosystem types, we chose to include BDOC measurements in our analysis despite a low
370 total number of measurements compared to DOC concentrations, and we consider this lower
371 sample size during our interpretation of results.

372 Filter size used in studies ranged from 0.15 – 0.7 μm . The majority of DOC
373 concentrations reported were determined using a filter size of 0.45 μm (58%), 0.7 μm was the
374 second most common filter size (21%), followed by 0.22 μm (14%). We identified eleven
375 different DOC extraction methods in total from both soils and water that are broadly grouped
376 into the following six extraction types; leaching, suction, grab, centrifuged, dialysis, and
377 potassium sulphate (K_2SO_4) extraction. Leaching includes the leaching and dry leaching of soil;
378 suction includes lysimeter, piezometer, pump, and rhizons; grab includes grab samples and ice
379 core extraction; and centrifuged, dialysis, and (K_2SO_4) extraction remain on their own. Suction
380 (42%), leaching (37%), and grab (14%) were the three most common extraction methods across
381 all samples. Leaching and suction extraction methods were used for 66% and 24%, respectively,

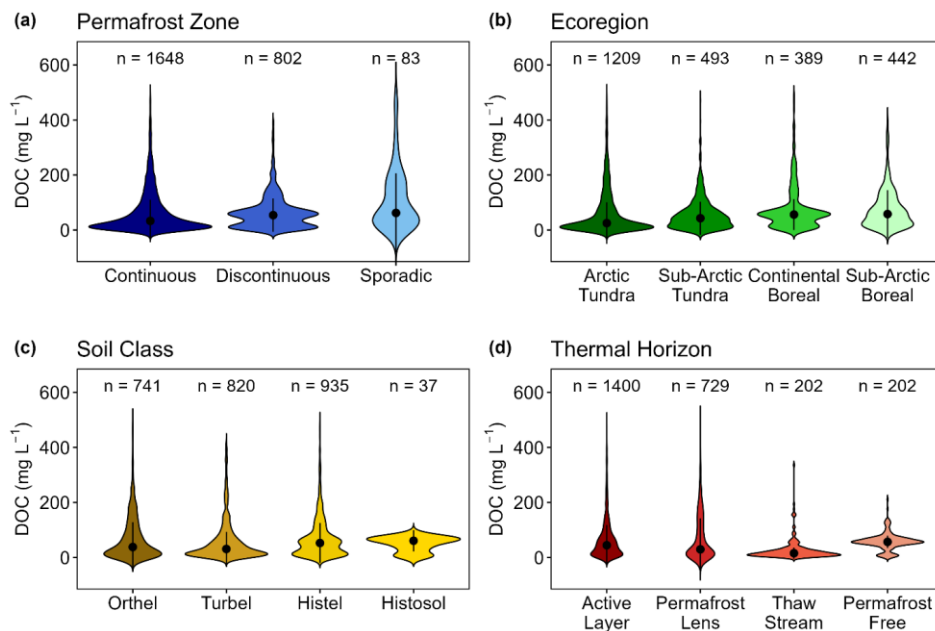
382 for all soil samples. For water samples, suction (65%) and grab (31%) were the most common
383 extraction methods. The most common measurement method to determine DOC concentrations
384 was by the combustion method (89%), followed by the persulphate (9%) and photometric (1%)
385 methods.

386 3.2 DOC concentrations and study regions

387 Upon inspection of DOC concentrations in the database, we determined that the data was
388 non-normally distributed. The DOC concentrations were skewed toward the lower end of our 0 –
389 500 mg L⁻¹ range; thus, we report median, upper, and lower quartiles below. Across all studies,
390 within the top 3 m of soil, the median DOC concentration was 41 ± 74 mg L⁻¹. DOC
391 concentrations were found to differ among the three permafrost zones (chi-square = 32, df = 2, *p*
392 < 0.001; Figure 2a). The highest median DOC concentrations were found within the sporadic
393 permafrost zone (n = 83; 62 ± 144 mg L⁻¹). The lowest median of 33 ± 77 mg L⁻¹ was found in
394 the continuous permafrost zone (n = 1,648), with the greatest density of samples having lower
395 DOC concentrations than observed in the violin plots of both the discontinuous and sporadic
396 (Figure 2a). This change in DOC concentration's along the latitudinal gradient of the permafrost
397 zonation was also seen in the latitudinal gradient associated with ecoregion, where Arctic Tundra
398 and Sub-Arctic Tundra are found at higher latitudes than both boreal ecoregions (chi-square =
399 78, df = 3, *p* < 0.001; Figure 2b). The highest DOC concentrations were found in the continental
400 boreal (n = 389; 56 ± 56 mg L⁻¹) and Sub-Arctic Boreal (n = 442; 58 ± 97 mg L⁻¹) ecoregions,
401 and lowest in the Arctic Tundra (n = 1,209; 25 ± 75 mg L⁻¹) and Sub-Arctic Tundra (n = 493; 43
402 ± 61 mg L⁻¹) ecoregions. Inspection of the distribution of DOC concentrations across the
403 ecoregions highlights that the Arctic Tundra ecoregion had the highest density of samples at the
404 lowest DOC concentration (Figure 2b).

405 These latitudinal differences are also reflected in the observed differences (chi-square =
406 20, df = 3, *p* < 0.001) in DOC concentrations found within different soil classes. The highest
407 DOC concentrations are found within organic rich Histosol (n = 37; 61 ± 39 mg L⁻¹) and Histel
408 soils (n = 935; 53 ± 72 mg L⁻¹; Figure 2c), with the distribution of the data from these soils types
409 having a higher density at greater DOC concentrations (Figure 2c). Histel and Histosol soils are
410 the main type of permafrost soil found within the sporadic and discontinuous permafrost zone

411 and both boreal ecoregions (Hugelius et al., 2014). Mineral rich Orthels ($n = 741$; $38 \pm 91 \text{ mg L}^{-1}$)
 412 ¹) and Turbels ($n = 820$; $31 \pm 62 \text{ mg L}^{-1}$), mineral permafrost soils that have experienced
 413 cryoturbation, had the lowest DOC concentrations. The median DOC concentrations found
 414 within the top 3 m of these soil classes represent <1% of the soil organic carbon stock found in
 415 the top 3 m of each soil class (Hugelius et al., 2014). DOC concentrations also differed within
 416 the thermal horizon of these different soil classes (chi-square = 91, $df = 3$, $p < 0.001$; Figure 2d).
 417 The highest DOC concentrations were found in permafrost free sites ($n = 202$; $57 \pm 22 \text{ mg L}^{-1}$),
 418 which were largely Histosol soils (19%) or Histel soils (74%) that have experienced thermokarst
 419 formation. In areas where permafrost was present, DOC concentrations were highest in the active
 420 layer ($n = 1,400$; $45 \pm 74 \text{ mg L}^{-1}$) and the permafrost lens ($n = 729$; $30 \pm 113 \text{ mg L}^{-1}$).



421
 422 Figure 2. Violin plots of DOC concentrations (mg L^{-1}) found in the top 3 m across (a) permafrost
 423 zones, (b) ecoregions, (c) soil classes, and (d) thermal horizons. (a) Dark to light blue shading
 424 represents the permafrost zones Continuous, Discontinuous, and Sporadic, according to Brown
 425 et al., (1997). (b) Dark to light green shading represents the ecoregions Arctic Tundra, Sub-
 426 Arctic Tundra, Continental Boreal, and Sub-Arctic Boreal, according to Olson et al., (2001). (c)
 427 Dark to light yellow shading represents the soil classes Histosol, Histel, Orthel, and Turbel,

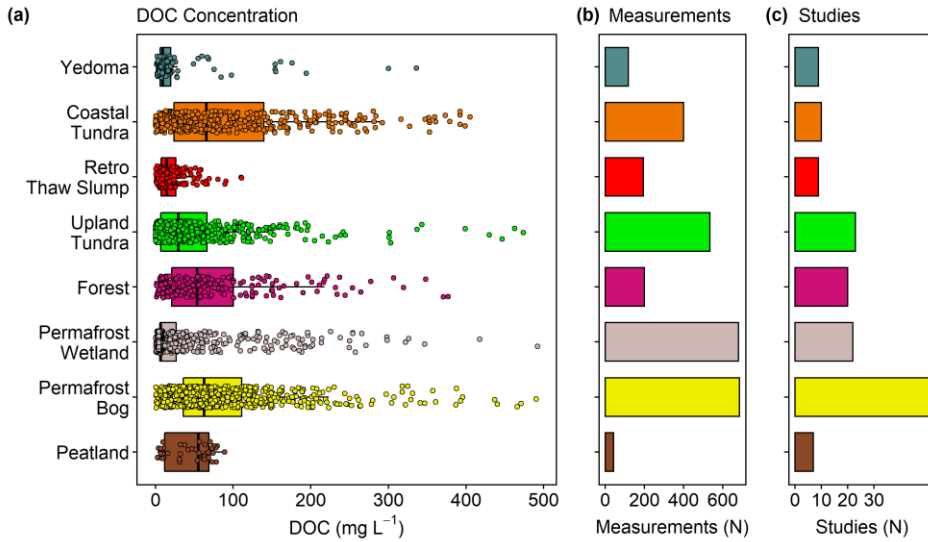
428 according to the USDA Soil Taxonomy (USDA, 1999). (d) Dark to light red shading represents
429 the thermal horizons Active Layer, Permafrost Lens, Thaw Stream, and Permafrost Free. Black
430 dots on each violin plot represents the median. Black vertical lines represent the interquartile
431 range with the upper and lower limits representing the 75th and 25th percentiles, respectively.
432 Either side of the black vertical line represents a kernel density estimation. This shape shows
433 the distribution of the data, with wider areas representing a higher probability that samples
434 within the database will have that DOC concentrations. The number of samples (n) found in
435 each sub-category is found above each corresponding violin plot.

436

437 *3.3 Trends in DOC concentrations across ecosystems*

438 Similar to other categorical variables (i.e. permafrost zone, ecoregion, soil class, and
439 thermal horizon data), DOC concentrations within each of the eight ecosystem types were found
440 to be non-normally distributed, with median values skewed toward the lower end of the 0 – 500
441 mg L⁻¹ range of concentrations (Figure S1). Permafrost bogs, upland tundra, and permafrost
442 wetlands were the most represented in the database with regards to DOC concentrations ([Table](#)
443 [S1](#)[Table S2](#)). The majority of permafrost bog measurements came from studies with field sites
444 within Canada (Figure 1; [Table S1](#)[Table S2](#)), as was the case for upland tundra and retrogressive
445 thaw slump DOC concentration data. The majority of permafrost wetland sample locations were
446 found in Russia, whereas the majority of the 414 coastal tundra sampling locations were in the
447 USA. The least represented ecosystem classes included the peatland ecosystem class, which is
448 not strictly a permafrost ecosystem as the other are, and the Yedoma ecosystem class (145 DOC
449 concentrations from 9 studies, [Table S1](#)[Table S2](#)). DOC concentrations differed significantly
450 across the eight ecosystem types (chi-square = 700, df = 7, $p < 0.001$; Figure 3). The highest
451 DOC concentrations were found in coastal tundra (66 ± 116 mg L⁻¹) and permafrost bogs ($63 \pm$
452 75 mg L⁻¹) ecosystems. The lowest DOC concentrations were found in permafrost wetlands ($7 \pm$
453 20 mg L⁻¹) and Yedoma ecosystems (9 ± 18 mg L⁻¹), both of which had only slightly lower
454 median DOC concentrations than retrogressive thaw slumps (15 ± 21 mg L⁻¹).

455



456

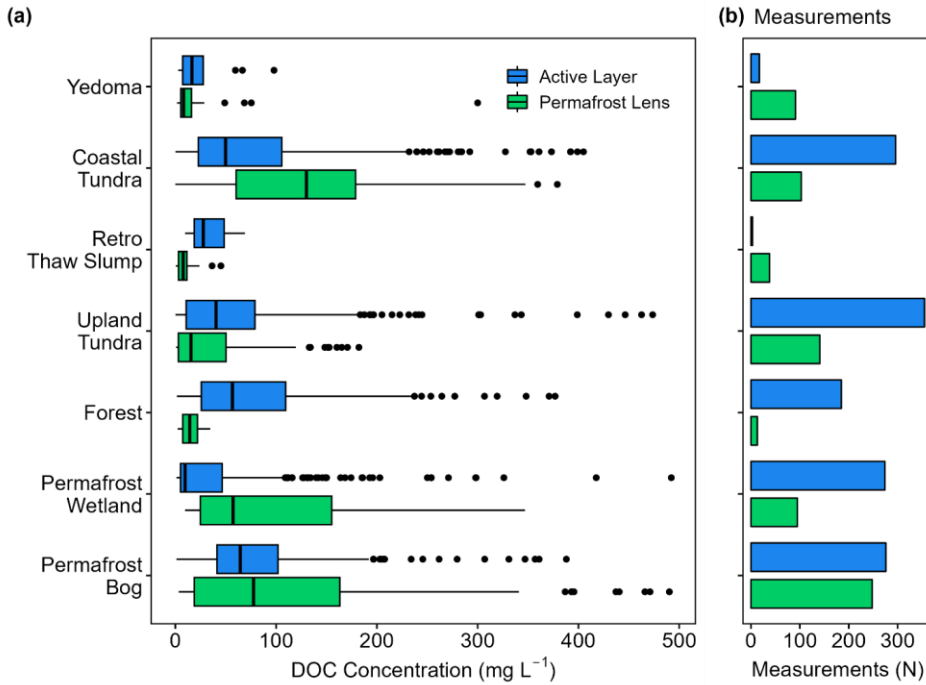
457 Figure 3. Boxplot and jitter plot of (a) DOC concentrations (mg L^{-1}), (b) the number of DOC
458 measurements, and (c) number of studies including DOC measurements were taken from the
459 top 3 m for each ecosystem type. Retro Thaw Slump = Retrogressive Thaw Slump. Boxes
460 represents the interquartile range (25 – 75%), with median shown as black horizontal line.
461 Whiskers extend to 1.5 times the interquartile range (distance between first and third quartile) in
462 each direction. Jitter points represent the concentration of each individual DOC measurement,
463 with random variation applied to each points location vertically in the plot, to avoid overplotting.
464 Yedoma = dark teal. Coastal Tundra = orange. Retro Thaw Slump = red. Upland Tundra =
465 green. Forest = purple. Permafrost Wetland = light pink. Permafrost bog = yellow. Peatland =
466 brown.

467

468 When grouping all DOC concentrations by ecosystem types and differentiating between
469 the active layer and permafrost lens thermal horizons, we found that DOC concentrations
470 differed between the active layer and permafrost lens for all ecosystems (ANCOVA: $F_{(1, 1277)} =$
471 $49.8, p < 0.001$), except for permafrost bogs (chi-square = 0.37, $df = 1, p = 0.5$) and Yedoma
472 (chi-square = 3.5, $df = 1, p = 0.06$) ecosystems (Figure 4). Within the permafrost lens thermal
473 horizon, the highest DOC concentrations were found in coastal tundra ($n = 103; 130 \pm 119 \text{ mg L}^{-1}$)
474 and permafrost bogs ($n = 248; 78 \pm 144 \text{ mg L}^{-1}$) sites, and lowest found in Yedoma sites ($n =$
475 $91; 8 \pm 10 \text{ mg L}^{-1}$). The highest active layer DOC concentrations were in permafrost bogs ($n =$

476 276; $64 \pm 61 \text{ mg L}^{-1}$) and forest ($n = 185$; $57 \pm 84 \text{ mg L}^{-1}$) sites, and lowest found in permafrost
 477 wetland sites ($n = 274$; $10 \pm 42 \text{ mg L}^{-1}$).

478



479

480 Figure 4 . Boxplot of (a) DOC concentrations (mg L^{-1}) and (b) the number of DOC
 481 measurements in the Active Layer and Permafrost Lens thermal horizons of each ecosystem
 482 type. Only DOC concentrations from ecosystems with these thermal horizons present is used,
 483 thus no permafrost-free sites are included. Retro Thaw Slump = Retrogressive Thaw Slump.
 484 Boxes represents the interquartile range (25 – 75%), with median shown as black horizontal
 485 line. Whiskers extend to 1.5 times the interquartile range (distance between first and third
 486 quartile) in each direction. Blue boxplots represent DOC concentrations in the active layer.
 487 Green boxplots represent DOC concentrations in the permafrost lens.

488

489 3.4 Effect of extraction and analysis methods on DOC concentrations

490 We found that DOC concentrations differed between filter sizes (ANOVA: $F_{(4, 2339)} =$
 491 $22.9, p < 0.001$) ~~acfo~~. The highest DOC median concentrations reported were filtered using 0.45

492 μm ($53 \pm 78 \text{ mg L}^{-1}$) and $0.22 \mu\text{m}$ ($42 \pm 54 \text{ mg L}^{-1}$) and lowest using $0.7 \mu\text{m}$ ($17 \pm 78 \text{ mg L}^{-1}$).
493 The majority of DOC concentrations were determined using 0.45 , 0.7 , and $0.22 \mu\text{m}$ filter sizes.
494 The trends observed in in DOC concentrations across study regions and ecosystems were also
495 found when exploring these trends for the three main filter sizes used (Table S2Table S3, S3).
496 Using 0.45 and $0.7 \mu\text{m}$ filter sizes, which represents 79% of all reported DOC concentrations, we
497 find that DOC concentrations are generally higher in the discontinuous and sporadic permafrost
498 zone, the two boreal ecoregions, Histel soils, and the active layer thermal horizons (Table
499 S2Table S3). Similarly, the highest DOC concentrations using these two most common filter
500 sizes were highest in permafrost bog and coastal tundra ecosystems (Table S3Table S4). Given
501 these similarities when considering and not considering filter size, and the large variation in
502 DOC concentrations within each filter size, we consider the effect of filter size on the trends
503 observed in DOC concentrations across study regions and ecosystems reported above (Figure 2,
504 3) to be minor.

505 DOC concentrations were found to be significantly different between samples subject to
506 the six broader groups of extraction method used (ANOVA: $F_{(5, 2518)} = 30.8, p < 0.001$), and
507 between water based and soil (solid) based extraction methods (ANOVA: $F_{(1, 2524)} = 182.1, p <$
508 0.001). The trends observed in in-DOC concentrations across study regions (Figure 2) and
509 ecosystems (Figure 3) were also found when exploring study region and ecosystem trends for the
510 three main DOC extraction methods used (Table S4Table S5, S5S6). We found that 93% of
511 DOC concentrations were determined using the suction (42%), leach (37%), and grab (14%)
512 extraction methods. Using these three most common approaches the highest DOC concentrations
513 across study regions (Table S4Table S5) and ecosystems (Table S5Table S6) were found in the
514 discontinuous and sporadic permafrost zone, the two boreal ecoregions, Histel soils, the active
515 layer thermal horizons, and in permafrost bog and coastal tundra ecosystems.

516 The different methods of measuring DOC concentrations also produced significantly
517 different DOC concentrations (ANOVA: $F_{(3, 2515)} = 36.2, p < 0.001$). The three most common
518 accounted for 99% of all DOC concentrations and were combustion, persulphate, and
519 photometric. Of these three combustion was the most common and used for 89% of DOC
520 measurements. The persulphate and photometric methods were not used in all study regions
521 (Table S6Table S7) and ecosystems (Table S7Table S8), thus comparison of all three methods is

522 not complete. Trends in DOC measured using the combustion and persulphate method (Table
523 S6, Table S7, S7) were similar to those found across study regions (Figure 2) and ecosystems
524 (Figure 3). This is unsurprising given that both of these methods account for 98% of all DOC
525 concentrations.

526 We consider the effect of filter size, extraction method, and method of DOC
527 measurement to be minor in determining trends in DOC concentrations across study regions and
528 ecosystems. We find that trends in DOC concentrations across study regions and ecosystems are
529 similar when you both consider and do not consider the methods used to determine those
530 concentrations. Also, the variability observed in DOC concentrations for each study region and
531 ecosystem remains high even when considering filter size, extraction method, and measurement
532 method. Thus, each method or approach similarly impacts DOC concentrations from each study
533 region and ecosystem, and cannot explain the DOC concentration variability observed within
534 each. However, these different approaches did have an impact on DOC concentrations. In this
535 study we did not focus on systematically testing the effect of filter sizes, extraction methods, or
536 DOC measurement methods. Our goal was to assess the concentration and mobilization of DOC
537 in terrestrial permafrost ecosystems across circumpolar regions and ecosystems. The assessment
538 of methods is outside the scope of our study. Rather, we compare DOC concentrations collected
539 from samples using a variety of these methods and suggest that future studies use this
540 information to decide on methods to be consistent with compiled measurements, thus far.

541 *3.5 Drivers of DOC concentrations*

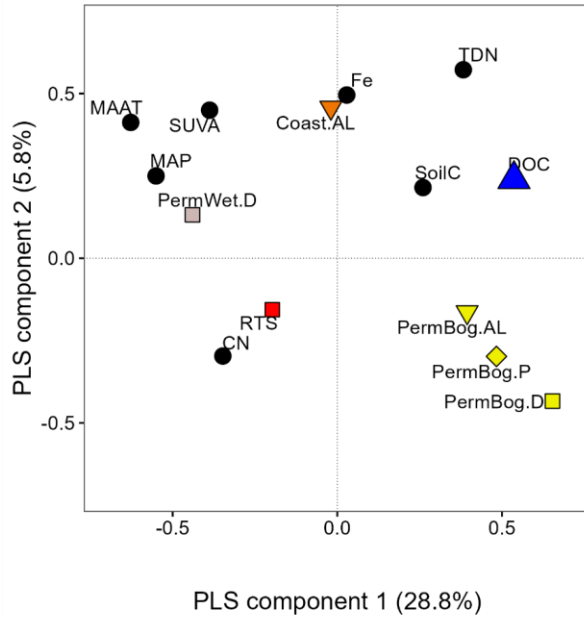
542 No continuous variables recorded in the dataset were available for all DOC concentration
543 database entries, with no sites containing data for all continuous variables. This limited our
544 ability to explore relationships between continuous environmental and ecological data and DOC
545 concentrations across the permafrost region. To address drivers of DOC concentrations across
546 the circumpolar permafrost region we used partial least squares regression (PLS) as it is tolerant
547 to missing values. Multiple PLS regressions were run using various combinations of continuous
548 and categorical data with similar model performance throughout. We chose the PLS to determine
549 the drivers of DOC concentrations using environmental continuous variables and ecosystem type
550 as this contained the lowest background correlation. The most parsimonious PLS regression

551 extracted 9 significant components, captured 79% variation of the predictor variables, and
552 explained 37% of the variance in DOC concentrations in the dataset. The majority of the
553 variance in DOC (35%) is explained along the first two axes of the model. The model was robust
554 and not overfitted as model predictability was moderate ($Q^2 = 0.35$) and background correlation
555 was low (0.006).

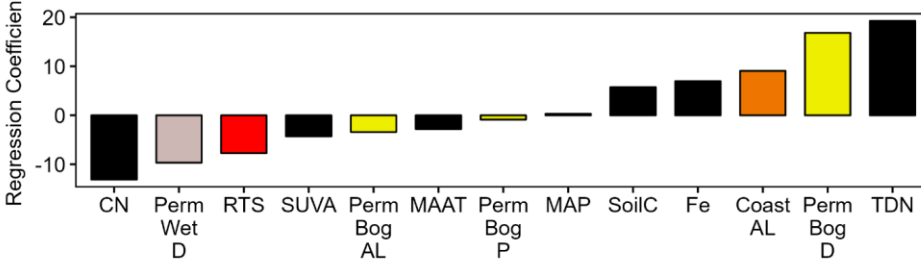
556 The PLS plot (Figure 5a) shows the correlation between DOC concentrations and
557 selected environmental and ecological variables for the first two axes of the model. The two
558 variables with the greatest positive and negative relationship with DOC concentrations were total
559 dissolved nitrogen content (mg L^{-1}) and C:N ratios, respectively (Figure 5b). The positive
560 relationship of DOC with total dissolved nitrogen and soil carbon content (SoilC), and negative
561 relationship with the specific UV absorbance at 254 nm (SUVA), may be a result of ecosystem
562 properties. The strong negative relationship with C:N ratios indicates that DOC concentrations
563 decrease with increased decomposition. Other than higher soil carbon content (SoilC) in
564 permafrost bogs, there was no clear or obvious observable trends in SoilC, TDN, C:N ratios, and
565 SUVA across ecosystem types (Figure S3). The PLS demonstrates that ecosystem type strongly
566 affects DOC concentrations, with DOC positively related with the highest ecosystems where the
567 highest DOC concentrations are observed, permafrost bogs and coastal tundra, and negatively
568 related to the lower DOC ecosystems, permafrost wetland and retrogressive thaw slumps (Figure
569 5). This negative relationship may be due to the higher latitudes these ecosystems are generally
570 found at, which is supported by the negative relationship with DOC and the climate indicators
571 mean annual temperature (MAAT) and mean annual precipitation (MAP). Additionally, it may
572 be due to the high number of thermokarst affected sites found within these ecosystem classes,
573 particularly retrogressive thaw slumps. There is a clear negative relationship between DOC
574 concentrations and disturbed permafrost wetlands, retrogressive thaw slumps, and permafrost
575 bogs.

576

(a)



(b)



577

578 Figure 5. Partial least squares regression (PLS) (a) loadings plot explaining 37% of the
 579 variability observed in DOC concentrations. (b) Bar plot of PLS regression coefficients showing
 580 the relative importance of each variable in predicting DOC concentrations. Regression
 581 coefficients on y-axis are normalized so their absolute sum is 100, with positive and negative
 582 values indicating the direction of the relationship. In the loadings plot squares depict ecosystem
 583 classes and the blue triangle represents DOC concentrations. Black circles in the (a) loadings
 584 plot and black bars in the (b) bar plot represent continuous environmental data that had at least
 585 20% coverage of DOC data. Continuous data variables are represented by the colour black. CN
 586 = carbon:nitrogen ratio. SUVA = the specific UV absorbance at 254 nm ($L\ mg\ C^{-1}\ m^{-1}$). MAP =

587 mean annual precipitation (mm). MAAT = mean annual temperature. SoilC = carbon content of
588 soil (g C kg^{-1}). TDN = total dissolved nitrogen (mg L^{-1}). Fe = dissolved iron (mg L^{-1}). PermWet.D
589 = disturbed permafrost wetland ecosystem class and is light pink (as in Figure 3) to represent
590 this ecosystem class. RTS = retrogressive thaw slump ecosystem class and is red (as in Figure
591 3) to represent this ecosystem class. Coast.AL = active layer of coastal tundra ecosystem class
592 and is orange. PermBog.AL = active layer of permafrost bog ecosystem class and is yellow.
593 PermBog.P = permafrost lens of permafrost bog ecosystem class and is yellow. PermBog.D =
594 disturbed permafrost bog ecosystem class and is yellow.

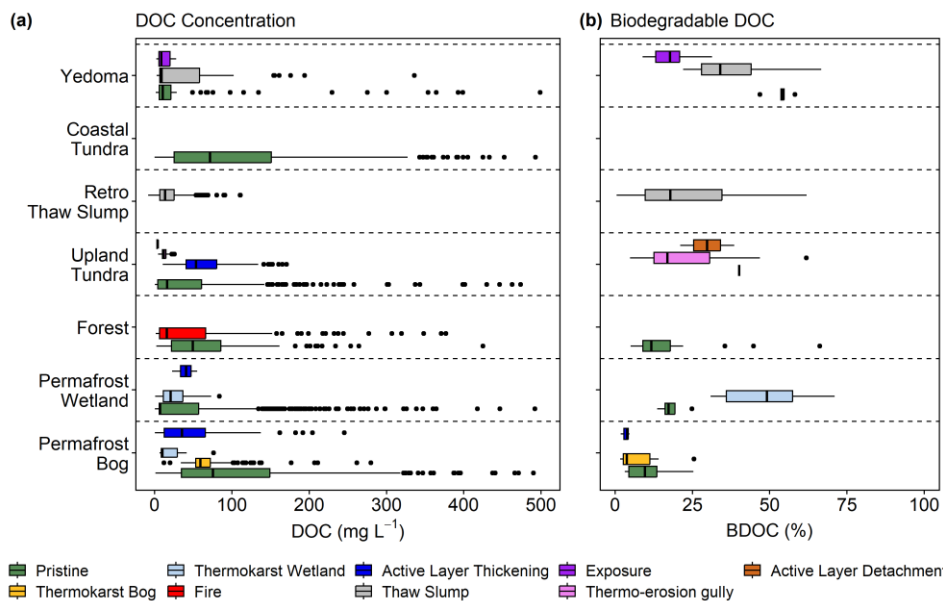
595 *3.6 Response and mobilization of DOC and BDOC to thermokarst formation*

596 The highest DOC concentrations were found in pristine permafrost bog ($n = 442$; $75 \pm$
597 112 mg L^{-1}) and coastal tundra ecosystems ($n = 427$; $72 \pm 126 \text{ mg L}^{-1}$; Figure 6a). No
598 thermokarst affected coastal tundra ecosystems were recorded within the dataset. Whereas, in
599 permafrost bogs DOC concentrations were found to differ across different thermokarst
600 disturbances (ANOVA: $F_{(3, 720)} = 23.04$, $p < 0.001$), with the lowest found in thermokarst
601 wetlands ($n = 16$; $10 \pm 21 \text{ mg L}^{-1}$). DOC concentrations were also found to differ between
602 thermokarst affected and pristine sites in upland tundra ecosystems (ANOVA: $F_{(3, 539)} = 5.91$, p
603 < 0.001). The highest DOC concentrations in upland tundra ecosystems were found in sites that
604 had experienced active layer thickening ($n = 142$; $53 \pm 39 \text{ mg L}^{-1}$), whereas the lowest were
605 found in sites that had experienced active layer detachment ($n = 6$; $4 \pm 2 \text{ mg L}^{-1}$). Pristine sites
606 had the highest DOC concentrations in both Yedoma ($n = 114$; $11 \pm 15 \text{ mg L}^{-1}$) and forest ($n =$
607 189 ; $49 \pm 64 \text{ mg L}^{-1}$) ecosystems. However, in permafrost wetland ecosystems pristine sites had
608 the lowest DOC concentrations ($n = 766$; $7 \pm 51 \text{ mg L}^{-1}$) with sites that were affected by both
609 thermokarst wetland formation ($n = 17$; $21 \pm 26 \text{ mg L}^{-1}$) and active layer thickening ($n = 12$; $41 \pm$
610 13 mg L^{-1}) having higher DOC concentrations.

611 Our database contained limited data regarding BDOC ($n = 146$), thus BDOC results
612 across ecosystems should be interpreted with caution. Due to limited data we have combined
613 BDOC over all incubation lengths when assessing BDOC between pristine and thermokarst sites
614 (Figure 6). BDOC was found to differ between thermokarst disturbances within ecosystem types
615 in only Yedoma (ANOVA: $F_{(2, 27)} = 23.09$, $p < 0.001$) and permafrost wetland (ANOVA: $F_{(1, 10)}$
616 $= 15.87$, $p < 0.001$) ecosystems. The highest BDOC was found in both of these ecosystem types
617 also, with 54% ($n = 5$) in pristine Yedoma sites and 49% ($n = 8$) in thermokarst wetland affected
618 permafrost wetland sites (Figure 6b), with the latter exhibiting the highest BDOC across all

619 permafrost affected sites followed by thaw slumps (18%, n = 11) in Yedoma ecosystems and
620 active layer thickening (40%, n = 1) in upland tundra sites. The lowest median BDOC of 4%
621 were seen in thermokarst bogs (n = 5) and active layer thickening (n = 3) affected sites, with
622 pristine sites experiencing BDOC of 9% (n = 15). However, not all ecosystem types in the
623 database had BDOC data for both pristine and disturbance sites. For example, only pristine sites
624 data was available for forests, whereas there was no pristine site data available for upland tundra
625 sites. No BDOC data was available for coastal tundra sites.

626 All ecosystem types that had BDOC data, reported BDOC observed following 40 – 90
627 incubation days, and this also corresponded to the highest BDOC values for each ecosystem type
628 (Figure S4). When comparing the greatest BDOC observed within this incubation length
629 window, we found that values varied across ecosystem type (ANOVA: $F_{(5, 131)} = 14.6, p <$
630 0.001). The highest loss rates were observed in Yedoma and permafrost wetland ecosystems,
631 whereas the lowest we observed in organic rich forest and permafrost bog ecosystems (Figure
632 S4). Forest (ANOVA: $F_{(1, 16)} = 2.31, p = 0.15$) and permafrost bog (ANOVA: $F_{(3, 24)} = 2.49, p =$
633 0.09) BDOC did not differ over incubation length, whereas Yedoma (ANOVA: $F_{(4, 25)} = 24.92, p$
634 < 0.001) and permafrost wetland (ANOVA: $F_{(1, 10)} = 15.87, p < 0.01$) did differ over time, with
635 their max occurring during this 40 – 90-day incubation length. This suggests that when incubated
636 for the same number of days, we would expect greater BDOC in Yedoma and permafrost
637 wetland ecosystems. Note, for this analysis BDOC values from all thermokarst and non-
638 thermokarst affected sites within an ecosystem type were included. Given the limited BDOC data
639 available we have compared BDOC across ecosystems in two ways. The first is using data from
640 all measurement days to assess BDOC across pristine and disturbed ecosystems (Figure 6b). The
641 second is assessing max BDOC within each ecosystem type, which includes pristine and
642 disturbed sites (Figure S4). Using both approaches we find that the highest BDOC is observed in
643 high-latitude Yedoma and permafrost wetland sites.



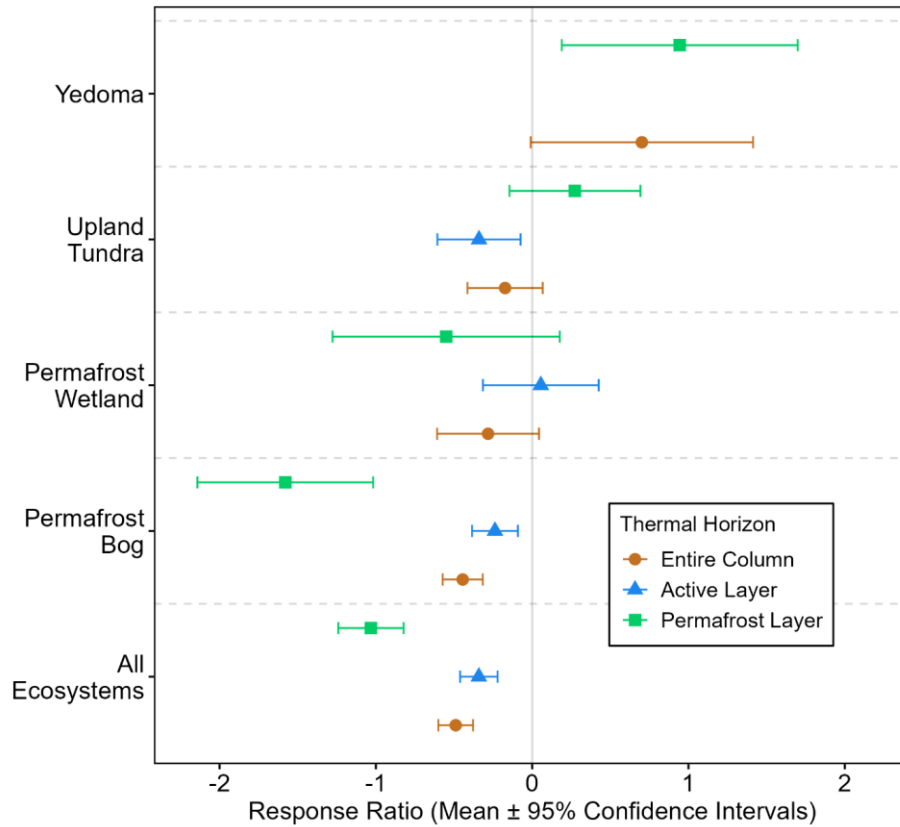
644

645 Figure 6. DOC concentrations (mg L^{-1}) and biodegradable DOC (BDOC; %) from the top 3 m
 646 following disturbance including data from both field based and incubation studies. (a) DOC
 647 concentrations from each ecosystem type following disturbance where data was available. (b)
 648 Biodegradable DOC (BDOC) from each ecosystem type following disturbance where data was
 649 available. BDOC loss was determined following 3 – 304 days of incubation. Data from different
 650 incubation lengths was combined due to low sample size. Retro Thaw Slump = Retrogressive
 651 Thaw Slump. Boxes represents the interquartile range (25 – 75%), with median shown as black
 652 horizontal line. Whiskers extend to 1.5 times the interquartile range (distance between first and
 653 third quartile) in each direction, with outlier data plotted individually as black dots. Note colours
 654 associated with boxplots in this figure are only relevant for this figure.

655 Response ratios comparing the change in DOC concentrations between pristine and
 656 thermokarst affected sites were calculated from our dataset from 108 studies using Eq. 1 (Figure
 657 7). Only 17 studies provided data for both pristine and thermokarst affected ecosystems, with 87
 658 papers providing DOC concentrations from pristine and 34 from thermokarst affected sites.
 659 When considering all ecosystems together we found that response ratios were negative,
 660 suggesting that DOC concentrations were higher in thermokarst affected sites compared to
 661 pristine sites (Figure 7). These negative response ratios were most evident in permafrost bogs,
 662 where they found throughout the entire column and individual thermal horizons. The greatest

663 increase in DOC concentrations following thermokarst was seen when comparing DOC
664 concentrations in the permafrost lens of permafrost bogs, and to a lesser extent permafrost
665 wetlands (Figure 7). Only in Yedoma ecosystems did we see positive response ratios throughout
666 the entire profile, suggesting a decrease in DOC concentrations following thermokarst formation
667 in Yedoma sites. This was also seen for DOC concentrations within the permafrost lens of
668 upland tundra sites, which include DOC concentrations from retrogressive thaw slumps and
669 thermo-erosion gullies in their thermokarst affected sites. The large confidence intervals for
670 some response ratios suggests high variability in the response of DOC concentrations to
671 thermokarst formation.

672



673

674 Figure 7. Response ratios of DOC concentrations from the top 3 m following thermokarst
 675 formation (calculated using Eq. 1). Response ratio means allow for relative comparison of
 676 changes in DOC following thermokarst formation between different ecosystem types. Negative
 677 values indicate lower DOC concentrations found in pristine ecosystems, whereas positive value
 678 indicates a decrease in DOC concentrations following thermokarst. Studies reporting DOC
 679 concentrations from Exposures, Retrogressive Thaw Slumps, and Thermo-Erosion Gullies from
 680 sites within the continuous permafrost zone were combined into the Upland Tundra ecosystem
 681 category. This did not include DOC concentrations from studies within the Yedoma permafrost
 682 domain (Strauss et al., 2021). Blue line represent DOC concentrations in the active layer, as per
 683 Figure 4. Green lines represent DOC concentrations in the permafrost lens, as per Figure 4.

684 Brown lines represent DOC concentrations from the entire column (i.e., both active layer and
685 permafrost lens).

686 **4. Discussion**

687 In this systematic review, we evaluated patterns of DOC concentrations in the top 3 m of
688 soil in terrestrial ecosystems across the northern circumpolar permafrost region based on results
689 from 111 studies and 2,845 DOC measurements. We focused on comparing concentrations of
690 DOC in soils across various geographical regions, ecological conditions, and disturbance types.
691 Our synthesis shows that median DOC concentrations across ecosystems range from 9 – 61 mg L⁻¹,
692 which represents similar albeit slightly higher DOC concentrations when compared to the
693 median DOC concentrations found in top soils of other land cover groups below 50°N (25 mg L⁻¹;
694 Langeveld et al., 2020), globally distributed lakes (6 mg L⁻¹; Sobek et al., 2007), and lakes
695 across the permafrost region (11 mg L⁻¹; Stolpmann et al., 2021). In general, we show that
696 organic soils have higher DOC concentrations than mineral soils, and that DOC concentrations
697 are positively related to total dissolved nitrogen concentrations and negatively to C:N ratios,
698 which corroborate previous findings of factors correlating with DOC concentrations (Aitkenhead
699 & McDowell, 2000; Lajtha et al., 2005). Overall, we found that properties associated with
700 ecosystem type are the main constraint on DOC concentrations. Furthermore, disturbance
701 through permafrost thaw has little impact on measured DOC concentrations, however this may
702 be due to the loss of biologically reactive DOC or the loss of an initially larger pulse of DOC
703 having been previously mobilised prior to the timing of sampling.

704 *4.1 Environmental factors influencing DOC*

705 Our database confirmed our first hypothesis that the highest DOC concentrations would be
706 found in organic rich soils. Previous synthesis efforts estimating global distributions of terrestrial
707 DOC concentrations have presented similar findings (Guo et al., 2020; Langeveld et al., 2020).
708 Both of these previous studies also show that some of the highest terrestrial DOC concentrations
709 are found within the northern circumpolar permafrost region, highlighting that these high DOC
710 concentrations found in organic rich permafrost soils are of global significance. Concentrations
711 of DOC in the top 3 m of soils closely mirrored stocks of SOC across the circumpolar permafrost
712 region (Hugelius et al., 2014). Organic rich Histosol and Histel soils contain the greatest SOC

713 per km², followed by Turbels and Orthels (Hugelius et al., 2014). The leaching of organic C from
714 soils act as a major source of DOC (Kalbitz et al., 2000; Marschner & Bredow, 2002), thus it is
715 not surprising that we find the highest DOC concentrations in the soil types with the greatest
716 quantities of SOC (Figure 2a). While the highest DOC concentrations are found within organic
717 rich soils, the amount of C found as DOC represent a small amount of the total SOC pool. Using
718 the current best estimates of Histel SOC stocks (Hugelius et al., 2020), the DOC pool represents
719 <1% of the total C stock in permafrost-affected peatlands as has been shown for both permafrost
720 and global soils (Guo et al., 2020; Prokushkin et al., 2008).

721 4.2 Variation in DOC across ecosystems

722 The accumulation of high DOC concentrations we show in permafrost bogs and permafrost
723 wetlands (Figure 3), is a result of the prevalence of cold and anoxic conditions throughout the
724 Holocene (Blodau, 2002). This leads to a reduction in microbial decomposition, and the
725 accumulation of both a large SOC (Hugelius et al., 2020) and DOC pool. Our results suggest that
726 the pristine permafrost bog and permafrost wetland DOC pool is relatively stable following
727 permafrost thaw (Figure 6, 7a). The lower DOC pool found in the active layer of permafrost
728 wetland (Figure 4a) may represent a potentially labile DOC pool (Figure 7a), but this is likely due
729 to fresh, plant derived inputs rather than the exposure and mineralization of previously frozen
730 organic matter (Figure 7a). Peatland vegetation, in particular *Sphagnum* mosses, produces litter
731 that has anti-microbial properties and is decay resistant (Hamard et al., 2019; Limpens, Bohlin,
732 & Nilsson, 2017), limiting the amount of SOC that is degraded and assimilated into the DOC
733 pool (Tfaily et al., 2013). This is further enhanced by the build-up of decomposition end products
734 and the thermodynamic constraint on decay observed in anoxic soils (Beer et al., 2008).
735 Permafrost has been continuously present in peatlands across the northern circumpolar
736 permafrost region for the past 6,000 years, with the greatest rates of permafrost formation
737 occurring within the past 3,000 years (Treat & Jones, 2018). Thus, a large proportion of the
738 organic matter found peatlands and wetlands in this region were present prior to permafrost
739 aggradation (i.e., permafrost formation), which indicates that permafrost formed epigenetically in
740 these areas. Permafrost aggradation impacts soil biogeochemical properties, leading to
741 potentially less decomposed organic matter with higher C/N ratios than non-permafrost
742 equivalent soils, particularly in permafrost wetlands (Treat et al., 2016). This can lead to the

743 build-up of high DOC concentrations that are vulnerable to potential mobilization following
744 thermokarst. Decomposition in epigenetic permafrost bogs following thermokarst has been
745 shown to be relatively slow (Heffernan et al., 2020; Manies et al., 2021), which further supports
746 our finding (Figure 6) that the large DOC pool found in these systems is relatively stable
747 following permafrost thaw.

748 Coastal tundra ecosystems had similarly high DOC concentrations to those found in
749 permafrost bogs (Figure 3a). Coastal tundra ecosystems represented the highest concentrations of
750 DOC in mineral permafrost soils, with the highest concentrations found in the permafrost lens
751 (Figure 4a). This is contrary to findings that deeper coastal permafrost consists of low organic
752 matter Pleistocene marine sediments (Bristol et al., 2021) and the proximity of the active layer to
753 vegetation inputs, although this productivity and inputs are vulnerable to projected climatic
754 warming and regional “browning” and “greening” (Lara et al., 2018). Recent work has shown
755 that DOC in the active layer within the coastal permafrost is more biodegradable than OC in the
756 permafrost lens (Speetjens et al., 2022) and a substantial proportion of organic carbon derived
757 from thawing coastal permafrost is vulnerable to mineralization upon thawing, particularly when
758 exposed to sea water (Tanski et al., 2021). Export of terrestrial coastal permafrost DOC directly
759 into the Arctic Ocean can significantly influence marine biogeochemical cycles and food webs
760 within the Arctic ocean (Bruhn et al., 2021). Arctic coasts are eroding at rates of up to 25 m yr⁻¹
761 (Fritz, Vonk, & Lantuit, 2017) and exporting large quantities of terrestrial organic matter export
762 directly to the ocean that is rapidly mineralized (Tanski et al., 2019). Enhanced DOC export from
763 these coastal tundra ecosystems may disrupt aquatic food webs through altering nutrient and
764 light supply, as has been shown for Swedish coastal systems (Peacock et al., 2022). These
765 coastal tundra sites represent a large DOC pool that is highly vulnerable to enhanced
766 mobilization and deserve further attention.

767 We found that DOC concentrations increased along a clear latitudinal gradient, from north to
768 south, in the remaining ecosystems characterised by mineral soils with an upper organic layer,
769 i.e., forests, upland tundra, and Yedoma. In forest ecosystems, the upper organic layer, and the
770 impact of soil temperature, moisture, and pH on SOC found there, strongly influences the
771 production, concentration, and composition of DOC (Neff & Hooper, 2002; Wickland et al.,
772 2007). Furthermore, the sorption of DOC to charcoal (Guggenberger et al., 2008), and high

773 lignin and phenolic input from vegetation (O'Donnell et al., 2016) produce a difficult to degrade
774 DOC pool, leading to the accumulation of the large DOC pool in the active layer (Figure 4a) this
775 ecosystem type. This trend with depth has also been observed in the vertical distribution of DOC
776 across global soils, with 50% of the DOC pool found in the top 0 – 30 cm (Guo et al., 2020).
777 While not included in the most parsimonious PLS model (Figure 5), Yedoma and upland tundra
778 ecosystems were found to negatively correlate with DOC concentrations (Figure S5). The
779 greatest proportions of OC and nutrients used for DOC production in these ecosystems are found
780 in shallow organic layers (Semenchuk et al., 2015; Wild et al., 2013). Beneath the upper organic
781 horizons in these mineral soils processes such as sorption of DOC to minerals and the formation
782 of Fe-DOC or Al-DOC complexes may remove DOC from the dissolved pool (Kawahigashi et
783 al., 2006) and mechanically protect it from mobilization (Gentsch et al., 2015). The majority of
784 vegetation and its leachates found in the permafrost region produce relatively stable DOC
785 consisting of lignin-derived compounds, highly aromatic polyphenolic compounds, and low
786 molecular weight organic acids (Chen et al., 2018; Drake et al., 2015; Ewing et al., 2015; Selvam
787 et al., 2017). While differences in the stability of different DOC source end-members have been
788 shown (MacDonald et al., 2021), differences in redox conditions are likely a major driver in
789 differences in the accumulation and mineralization of DOC across permafrost ecosystem types
790 (Mohammed et al., 2022).

791 *4.3 Vulnerability of DOC to enhanced mobilization following thermokarst*

792 We define DOC mobilization as DOC lost from an ecosystem either via export or
793 degradation. Our second hypothesis that permafrost thaw would lead to enhanced mobilization of
794 DOC cannot be fully supported by the findings from this database. Using our chosen systematic
795 approach and focusing on data from terrestrial ecosystems, our database was limited to 3 studies
796 which represented <1% of the DOC concentration data. Several previous studies have detailed
797 the export of DOC in Arctic inland waters, see Table 2 in Ma et al., (2019). These studies were
798 excluded using our systematic approach (Table 1 and 2) as they do not directly measure DOC
799 export from a terrestrial ecosystem, rather they determine the quantity of terrestrial derived DOC
800 found in inland waters. This is a key distinction, as by not quantifying the export rates for
801 terrestrial ecosystems the net ecosystem carbon balance and vulnerability to enhanced export
802 may not be assessed. We acknowledge the limitation in our approach regarding the inclusion of

803 DOC export data. Thus, this database cannot be used to determine how permafrost thaw will
804 influence DOC export from terrestrial ecosystems within the northern circumpolar permafrost
805 region. However, we identify this lack of export data from terrestrial permafrost ecosystems as a
806 key knowledge gap in our current understanding of the permafrost carbon pool. Currently, Arctic
807 rivers are estimated to export 25 – 36 Tg DOC year⁻¹ (Amon et al., 2012; Holmes et al., 2012),
808 with this being dominated by modern carbon sources (Estop-Aragonés et al., 2020), most likely
809 derived from the top 1 m of terrestrial ecosystems. Using current best estimates of the areal
810 extent and soil organic carbon stores in the top 1 m of Histosols, Histels, Orthels and Turbels
811 (Hugelius et al., 2014), and if we assume that the DOC pool represents ~1% of the SOC pool, we
812 estimate that <1% of the current DOC pool found in the top 1 m of Histosols, Histels, Orthels
813 and Turbels is exported annually to Arctic rivers. Quantifying the proportion of these DOC pools
814 annually lost, and particularly the proportions lost in headwater streams while being exported to
815 Arctic rivers, is vital to assess the importance of the mobilization of the terrestrial permafrost
816 DOC pool.

817 Our calculated response ratios (Figure 7) for all ecosystems, indicating the difference in DOC
818 concentrations between pristine and permafrost thaw affected sites, partly supports of our second
819 hypothesis that disturbance would lead to increased export and biodegradability of DOC. The
820 increase in DOC following thaw observed in permafrost bogs is likely due to increased inputs
821 due to increased runoff and shifts in vegetation following permafrost thaw (Burd, Estop-
822 Aragonés, Tank, & Olefeldt, 2020), enhanced release of DOC (Loiko et al., 2017), a relatively
823 stable soil organic carbon pool at depth due to several millennia of microbial processing (Manies
824 et al., 2021), the prevalence of anoxic conditions, and the potential hydrological isolation of
825 thermokarst bogs (Quinton, Hayashi, & Pietroniro, 2003). While not included in our analysis,
826 DOC found near the surface of the permafrost lens in forest ecosystems has been shown to be
827 more biodegradable than DOC found in the active layer (Wickland et al., 2018), and may
828 represent a decrease in DOC following thermokarst not captured here. Our findings of limited
829 mobilization of permafrost bog DOC upon thawing are supported by the findings that the ¹⁴C
830 signature of DOC in Arctic rivers is dominated by modern sources (Estop-Aragonés et al., 2020).
831 However, individual studies have determined that thawing may release a large pool of permafrost
832 peatland DOC into aquatic networks (Lim et al., 2021). We do see a reduction in DOC

833 concentrations in thermokarst affected sites at the higher latitude Yedoma, upland tundra, and
834 permafrost wetland ecosystems. This reduction in DOC concentrations in these ecosystems may
835 be due to the greater biodegradability and lability of the DOC found there (Figure 6b),
836 supporting our third hypothesis that the most biodegradable DOC would be found in higher
837 latitude ecosystems. Permafrost DOC in higher latitude ecosystems, particularly Yedoma
838 ecosystems, is characterised by syngenetic permafrost aggradation which have not undergone
839 centuries to millennia of soil formation and microbial processes, have been shown contain a
840 greater proportion of low oxygen, aliphatic compounds and labile substrates (Ewing et al.,
841 2015b; MacDonald et al., 2021). This leads to a greater biolability and rapid mineralization of
842 DOC (Vonk et al., 2015), potentially causing the reduction in DOC concentrations observed
843 following thaw. If this hypothesis is to be found true across all high latitude ecosystems with
844 further data, it further highlights the vulnerability of the large DOC pool found in coastal tundra
845 ecosystems.

846 In this study, we focus on the dissolved fraction of the OC pool, however the particulate
847 fraction should also be considered when discussing the mobilization of terrestrial OC in
848 permafrost landscapes. In boreal freshwater networks, particulate organic carbon (POC)
849 represents a small but highly labile fraction of terrestrially derived OC exported to the fluvial
850 network (Attemeyer et al., 2018). The degradation of permafrost derived POC is much slower
851 than that of POC in the boreal freshwater network and POC derived from younger sources along
852 the riverbank (Shakil, Tank, Kokelj, Vonk, & Zolkos, 2020). The DOC pool in Arctic
853 freshwaters is dominated by modern terrestrial sources (Estop-Aragonés et al., 2020), whereas
854 the POC pool has been shown to be dominated by older sources in both permafrost peatland
855 dominated areas (Wild et al., 2019), following the formation of retrogressive thaw slumps
856 (Keskitalo et al., 2021), and in thermokarst affected periglacial streams (Bröder et al., 2022).
857 This older POC has been shown to accumulate following export due to low lability and
858 degradation and mineral association, which suggests that upon thermokarst formation, previously
859 frozen OC exported in the particulate phase is not readily consumed by microbes and that
860 permafrost derived DOC is the more labile fraction of exported terrestrial OC.

861 *4.4 Future considerations for study design*

862 Determining the fate of mobilized terrestrial DOC in both permafrost thaw affected, and
863 pristine sites should be prioritized in future studies to constrain current estimates of the
864 permafrost C climate feedback. There are large spatial gaps in the database, particularly in areas
865 with large stock of permafrost C such as the Hudson Bay Lowlands and Mackenzie River Basin,
866 both in Canada and two of the three largest deposits of permafrost peatland C in the circumpolar
867 permafrost region (Olefeldt et al., 2021). Similarly, coastal tundra sites, which along with
868 permafrost bog represent the ecosystems with the highest DOC concentrations, were sampled
869 only along the northern shoreline of Alaska and the Yukon (USA and Canada, respectively;
870 [Table S1](#)+[Table S2](#)). From our analysis of this database, we determine that DOC mobilization is
871 poorly understood for terrestrial permafrost ecosystems. To address this, the two main needs of
872 future studies are 1) more direct estimates of DOC fluxes and export from terrestrial ecosystems
873 into aquatic ecosystems, and 2) more DOC degradation (BDOC) and mineralization studies. Our
874 results suggest that the high concentrations of DOC in permafrost bogs remains relatively stable
875 upon thermokarst formation, although individual studies do indicate that thawing peat may
876 provide a reactive source of DOC (Panneer Selvam et al., 2017). The database did not include
877 any studies that reported on the mineralization of DOC from coastal tundra sites, thus we are
878 unable to comment on the stability of the high DOC concentrations found in this ecosystem type.
879 Further sampling and assessing the mineralization of DOC is required to characterize the
880 potential pool of vulnerable DOC in areas with high DOC concentrations. Overall, our database
881 and systematic approach only included 5 studies (Olefeldt & Roulet, 2012, 2014; Olefeldt et al.,
882 2012; Prokushkin et al., 2006; Prokushkin et al., 2005) that explicitly reported rates of DOC
883 discharge, export, or fluxes from terrestrial ecosystems into the fluvial network. Given the
884 importance of terrestrial DOC as a source for CO₂ production within the aquatic network
885 (Weyhenmeyer et al., 2012), and the findings that previously frozen DOC is being exported to
886 the freshwater network (Estop-Aragones et al., 2020), improved estimates of the quantity of
887 terrestrial DOC being exported is essential to determine the potential aquatic greenhouse gas
888 fluxes derived from the mineralization of terrigenous organic matter. To improve current
889 estimates of the permafrost C feedback further studies are needed to determine how much DOC
890 is laterally exported from terrestrial ecosystems, and the mineralization potential of this DOC
891 along the terrestrial-freshwater-aquatic continuum.

892 Lastly, we suggest that future studies should consider a standardization of methods and
893 approached used to determine DOC concentrations for better comparison across studies. In
894 constructing this database we identified three different filter sizes, eleven different extraction
895 procedures, and four different measurement methods. The most common filter size used was
896 0.45 μm and this has previously been described as the cut off to separate DOC from colloid
897 materials (Thurman 1985; Bolan et al., 1999). In extracting DOC concentrations from soils the
898 mostly commonly used approach (70% of all soil samples) was via soil leaching with no
899 chemical treatment of the soils, although some added filtered water to promote leaching. From
900 the seven approaches identified to extract water samples from terrestrial sites in determining
901 DOC, 48% of samples were collected using a variety of suction devices and 46% done via grab
902 samples. Of the four DOC measurements methods the most common approach was by
903 combustion, with 90% of all DOC concentrations measured using this approach. As such, in
904 order to continue measuring DOC concentrations in terrestrial permafrost ecosystems using the
905 most consistent approach we suggest using 0.45 μm filters, extracting pore water via some type
906 of sucking device or soils via leaching, and using a combustion based method to determine DOC
907 concentrations

908 **Data availability**

909 [All data is freely and publicly available at https://doi.org/10.17043/heffernan-2024-doc-1](https://doi.org/10.17043/heffernan-2024-doc-1)

910 ~~All data will be made freely and publicly available on an online repository prior to publication~~

911 **Author contributions**

912 LH, DK, and LT designed and planned the systematic review approach; LH built the database.
913 LH and DK analyzed the data; LH wrote the manuscript draft; DK and LT edited and reviewed
914 the manuscript.

915 **Competing interests**

916 The authors declare that they have no conflict of interest.

917 **Acknowledgements**

918 We thank Konstantinos Vaziourakis, Mona Abbasi, Elizabeth Jakobsson, Marloes Groeneveld,
919 Sarah Shakil, and Jeffrey Hawkes for helpful discussions throughout the development and
920 writing of this manuscript.

921 **Financial support**

922 This work was supported by the Knut and Alice Wallenberg Foundation. DK was funded from
923 the Swedish National Science Foundation (VR 2020-03249).

924 **References (in text)**

- 925 Abbott, B. W., Larouche, J. R., Jones, J. J. B., Bowden, W. B., & Balsler, A. W. (2014). From
926 Thawing and Collapsing Permafrost. *Journal of Geophysical Research: Biogeosciences*,
927 *119*, 2049–2063. <https://doi.org/10.1002/2014JG002678>. Received
- 928 Aitkenhead, J. A., & McDowell, W. H. (2000). Soil C:N ratio as a predictor of annual riverine
929 DOC flux at local and global scales. *Global Biogeochemical Cycles*, *14*(1).
930 <https://doi.org/10.1029/1999GB900083>
- 931 Amon, R. M. W., Rinehart, A. J., Duan, S., Louchouart, P., Prokushkin, A., Guggenberger, G.,
932 ... Zhulidov, A. V. (2012). Dissolved organic matter sources in large Arctic rivers.
933 *Geochimica et Cosmochimica Acta*, *94*, 217–237.
934 <https://doi.org/https://doi.org/10.1016/j.gca.2012.07.015>
- 935 Andersen, C.M. and Bro, R. (2010), Variable selection in regression—a tutorial. *J.*
936 *Chemometrics*, *24*: 728-737. <https://doi.org/10.1002/cem.1360>
- 937 Andresen, C. G., Lawrence, D. M., Wilson, C. J., McGuire, A. D., Koven, C., Schaefer, K.,
938 Jafarov, E., Peng, S., Chen, X., Gouttevin, I., Burke, E., Chadburn, S., Ji, D., Chen, G.,
939 Hayes, D., and Zhang, W.: Soil moisture and hydrology projections of the permafrost region
940 – a model intercomparison, *The Cryosphere*, *14*, 445–459, [https://doi.org/10.5194/tc-14-](https://doi.org/10.5194/tc-14-445-2020)
941 [445-2020](https://doi.org/10.5194/tc-14-445-2020), 2020.
- 942 Arksey, H., & O'Malley, L. (2005). Scoping studies: Towards a methodological framework.
943 *International Journal of Social Research Methodology: Theory and Practice*, *8*(1).
944 <https://doi.org/10.1080/1364557032000119616>
- 945 Attermeyer, K., Catalán, N., Einarsdottir, K., Freixa, A., Groeneveld, M., Hawkes, J. A., ...
946 Tranvik, L. J. (2018). Organic Carbon Processing During Transport Through Boreal Inland
947 Waters: Particles as Important Sites. *Journal of Geophysical Research: Biogeosciences*,
948 *123*(8). <https://doi.org/10.1029/2018JG004500>
- 949 Beckebanze, L., Runkle, B. R. K., Walz, J., Wille, C., Holl, D., Helbig, M., ... Kutzbach, L.

- 950 (2022). Lateral carbon export has low impact on the net ecosystem carbon balance of a
951 polygonal tundra catchment. *BIOGEOSCIENCES*, 19(16), 3863–3876.
952 <https://doi.org/10.5194/bg-19-3863-2022>
- 953 Beer, J., Lee, K., Whiticar, M., & Blodau, C. (2008). Geochemical controls on anaerobic organic
954 matter decomposition in a northern peatland. *Limnology and Oceanography*, 53(4), 1393–
955 1407. <https://doi.org/10.4319/lo.2008.53.4.1393>
- 956 Biester, H., Knorr, K. H., Schellekens, J., Basler, A., & Hermanns, Y. M. (2014). Comparison of
957 different methods to determine the degree of peat decomposition in peat bogs.
958 *Biogeosciences*. <https://doi.org/10.5194/bg-11-2691-2014>
- 959 Blodau, C. (2002). Carbon cycling in peatlands — A review of processes and controls.
960 *Environmental Reviews*, 10(2), 111–134. <https://doi.org/10.1139/a02-004>
- 961 Bolan, N.S., Baskaran, S., Thiagarajan, S. (1999). Methods of Measurement of Dissolved
962 Organic Carbon of Plant Origin in Soils, Manures, Sludges and Stream Water. In: Linskens,
963 H.F., Jackson, J.F. (eds) Analysis of Plant Waste Materials. Modern Methods of Plant
964 Analysis, vol 20. Springer, Berlin, Heidelberg. [https://doi.org/10.1007/978-3-662-03887-
965 1_1](https://doi.org/10.1007/978-3-662-03887-1_1)
- 966 Bristol, E. M., Connolly, C. T., Lorenson, T. D., Richmond, B. M., Ilgen, A. G., Choens, R. C.,
967 ... McClelland, J. W. (2021). Geochemistry of Coastal Permafrost and Erosion-Driven
968 Organic Matter Fluxes to the Beaufort Sea Near Drew Point, Alaska. *Frontiers in Earth
969 Science*, 8. <https://doi.org/10.3389/feart.2020.598933>
- 970 Bröder, L., Hirst, C., Opfergelt, S., Thomas, M., Vonk, J. E., Haghypour, N., ... Fouché, J.
971 (2022). Contrasting Export of Particulate Organic Carbon From Greenlandic Glacial and
972 Nonglacial Streams. *Geophysical Research Letters*, 49(21).
973 <https://doi.org/10.1029/2022GL101210>
- 974 Brown, J., Ferrians Jr., O. J., Heginbottom, J. A., & Melnikov, E. S. (1997). Circum-Arctic map
975 of permafrost and ground ice conditions. *USGS Numbered Series*, 1.
976 <https://doi.org/10.1016/j.jallcom.2010.03.054>
- 977 Bruhn, A. D., Stedmon, C. A., Comte, J., Matsuoka, A., Speetjens, N. J., Tanski, G., ... Sjöstedt,
978 J. (2021). Terrestrial Dissolved Organic Matter Mobilized From Eroding Permafrost
979 Controls Microbial Community Composition and Growth in Arctic Coastal Zones.
980 *Frontiers in Earth Science*, 9. <https://doi.org/10.3389/feart.2021.640580>
- 981 Burd, K., Estop-Aragonés, C., Tank, S. E., & Olefeldt, D. (2020). Lability of dissolved organic
982 carbon from boreal peatlands: interactions between permafrost thaw, wildfire, and season.
983 *Canadian Journal of Soil Science*, 13(February), 1–13. [https://doi.org/10.1139/cjss-2019-
0154](https://doi.org/10.1139/cjss-2019-
984 0154)
- 985 Camill, P. (2005). Permafrost thaw accelerates in boreal peatlands during late-20th century

- 986 climate warming. *Climatic Change*, 68(1–2), 135–152. [https://doi.org/10.1007/s10584-005-](https://doi.org/10.1007/s10584-005-4785-y)
987 4785-y
- 988 Chanton, J. P., Glaser, P. H., Chasar, L. S., Burdige, D. J., Hines, M. E., Siegel, D. I., ... Cooper,
989 W. T. (2008). Radiocarbon evidence for the importance of surface vegetation on
990 fermentation and methanogenesis in contrasting types of boreal peatlands. *Global*
991 *Biogeochemical Cycles*, 22(4), 1–11. <https://doi.org/10.1029/2008GB003274>
- 992 Chen, H., Yang, Z., Chu, R. K., Tolic, N., Liang, L., Graham, D. E., ... Gu, B. (2018). Molecular
993 Insights into Arctic Soil Organic Matter Degradation under Warming. *ENVIRONMENTAL*
994 *SCIENCE & TECHNOLOGY*, 52(8), 4555–4564. <https://doi.org/10.1021/acs.est.7b05469>
- 995 Chong, I. G., & Jun, C. H. (2005). Performance of some variable selection methods when
996 multicollinearity is present. *Chemometrics and Intelligent Laboratory Systems*, 78(1).
997 <https://doi.org/10.1016/j.chemolab.2004.12.011>
- 998 Connon, R. F., Quinton, W. L., Craig, J. R., & Hayashi, M. (2014). Changing hydrologic
999 connectivity due to permafrost thaw in the lower Liard River valley, NWT, Canada.
1000 *Hydrological Processes*, 28(14). <https://doi.org/10.1002/hyp.10206>
- 1001 Dean, J. F., Meisel, O. H., Rosco, M. M., Marchesini, L. B., Garnett, M. H., Lenderink, H., ...
1002 Dolman, A. J. (2020). East Siberian Arctic inland waters emit mostly contemporary carbon.
1003 *NATURE COMMUNICATIONS*, 11(1). <https://doi.org/10.1038/s41467-020-15511-6>
- 1004 Drake, T. W., Wickland, K. P., Spencer, R. G. M., McKnight, D. M., & Striegl, R. G. (2015).
1005 Ancient low-molecular-weight organic acids in permafrost fuel rapid carbon dioxide
1006 production upon thaw. *PROCEEDINGS OF THE NATIONAL ACADEMY OF SCIENCES*
1007 *OF THE UNITED STATES OF AMERICA*, 112(45), 13946–13951.
1008 <https://doi.org/10.1073/pnas.1511705112>
- 1009 Ernakovich, J. G., Lynch, L. M., Brewer, P. E., Calderon, F. J., & Wallenstein, M. D. (2017).
1010 Redox and temperature-sensitive changes in microbial communities and soil chemistry
1011 dictate greenhouse gas loss from thawed permafrost. *BIOGEOCHEMISTRY*, 134(1–2),
1012 183–200. <https://doi.org/10.1007/s10533-017-0354-5>
- 1013 Estop-Aragones, C., Olefeldt, D., Abbott, B. W., Chanton, J. P., Czimeczik, C. I., Dean, J. F., ...
1014 Anthony, K. W. (2020). Assessing the Potential for Mobilization of Old Soil Carbon After
1015 Permafrost Thaw: A Synthesis of C-14 Measurements From the Northern Permafrost
1016 Region. *GLOBAL BIOGEOCHEMICAL CYCLES*, 34(9).
1017 <https://doi.org/10.1029/2020GB006672>
- 1018 Estop-Aragónés, Cristian, Czimeczik, C. I., Heffernan, L., Gibson, C., Walker, J. C., Xu, X., &
1019 Olefeldt, D. (2018). Respiration of aged soil carbon during fall in permafrost peatlands
1020 enhanced by active layer deepening following wildfire but limited following thermokarst.
1021 *Environmental Research Letters*, 13(8). <https://doi.org/10.1088/1748-9326/aad5f0>
- 1022 Ewing, S. A., Paces, J. B., O'Donnell, J. A., Jorgenson, M. T., Kanevskiy, M. Z., Aiken, G. R.,

- 1023 ... Striegl, R. (2015a). Uranium isotopes and dissolved organic carbon in loess permafrost:
 1024 Modeling the age of ancient ice. *GEOCHIMICA ET COSMOCHIMICA ACTA*, 152, 143–
 1025 165. <https://doi.org/10.1016/j.gca.2014.11.008>
- 1026 Ewing, S. A., Paces, J. B., O'Donnell, J. A., Jorgenson, M. T., Kanevskiy, M. Z., Aiken, G. R.,
 1027 ... Striegl, R. (2015b). Uranium isotopes and dissolved organic carbon in loess permafrost:
 1028 Modeling the age of ancient ice. *Geochimica et Cosmochimica Acta*, 152, 143–165.
 1029 <https://doi.org/10.1016/j.gca.2014.11.008>
- 1030 Fouché, J., Christiansen, C. T., Lafrenière, M. J., Grogan, P., & Lamoureux, S. F. (2020).
 1031 Canadian permafrost stores large pools of ammonium and optically distinct
 1032 dissolved organic matter. *Nature Communications*, 11(1), 4500.
 1033 <https://doi.org/10.1038/s41467-020-18331-w>
- 1034 Fritz, M., Vonk, J. E., & Lantuit, H. (2017). Collapsing Arctic coastlines. *Nature Climate*
 1035 *Change*. <https://doi.org/10.1038/nclimate3188>
- 1036 Gentsch, N., Mikutta, R., Shibistova, O., Wild, B., Schnecker, J., Richter, A., ... Guggenberger,
 1037 G. (2015). Properties and bioavailability of particulate and mineral-associated organic
 1038 matter in Arctic permafrost soils, Lower Kolyma Region, Russia. *European Journal of Soil*
 1039 *Science*, 66(4). <https://doi.org/10.1111/ejss.12269>
- 1040 Guggenberger, G., & Zech, W. (1993). Dissolved organic carbon control in acid forest soils of
 1041 the Fichtelgebirge (Germany) as revealed by distribution patterns and structural
 1042 composition analyses. *Geoderma*, 59(1–4). [https://doi.org/10.1016/0016-7061\(93\)90065-S](https://doi.org/10.1016/0016-7061(93)90065-S)
- 1043 Guggenberger, Georg, Rodionov, A., Shibistova, O., Grabe, M., Kasansky, O. A., Fuchs, H., ...
 1044 Flessa, H. (2008). Storage and mobility of black carbon in permafrost soils of the forest
 1045 tundra ecotone in Northern Siberia. *Global Change Biology*, 14(6), 1367–1381.
 1046 <https://doi.org/10.1111/j.1365-2486.2008.01568.x>
- 1047 Guo, Z., Wang, Y., Wan, Z., Zuo, Y., He, L., Li, D., ... Xu, X. (2020). Soil dissolved organic
 1048 carbon in terrestrial ecosystems: Global budget, spatial distribution and controls. *Global*
 1049 *Ecology and Biogeography*, 29(12). <https://doi.org/10.1111/geb.13186>
- 1050 Hamard, S., Robroek, B. J. M., Allard, P. M., Signarbieux, C., Zhou, S., Saesong, T., ... Jassey,
 1051 V. E. J. (2019). Effects of Sphagnum Leachate on Competitive Sphagnum Microbiome
 1052 Depend on Species and Time. *Frontiers in Microbiology*, 10.
 1053 <https://doi.org/10.3389/fmicb.2019.02042>
- 1054 Hansen, A. M., Kraus, T. E. C., Pellerin, B. A., Fleck, J. A., Downing, B. D., & Bergamaschi, B.
 1055 A. (2016). Optical properties of dissolved organic matter (DOM): Effects of biological and
 1056 photolytic degradation. *Limnology and Oceanography*, 61(3), 1015–
 1057 1032. <https://doi.org/10.1002/lno.10270>
- 1058 Heffernan, L., Cavaco, M. A., Bhatia, M. P., Estop-Aragonés, C., Knorr, K.-H., & Olefeldt, D.

- 1059 (2022). High peatland methane emissions following permafrost thaw: enhanced acetoclastic
 1060 methanogenesis during early successional stages. *Biogeosciences*, 19(12).
 1061 <https://doi.org/10.5194/bg-19-3051-2022>
- 1062 Heffernan, L., Estop-Aragónés, C., Knorr, K.-H., Talbot, J., & Olefeldt, D. (2020). Long-term
 1063 impacts of permafrost thaw on carbon storage in peatlands: deep losses offset by surficial
 1064 accumulation. *Journal of Geophysical Research: Biogeosciences*, 2011(2865),
 1065 e2019JG005501. <https://doi.org/10.1029/2019JG005501>
- 1066 Heslop, J. K., Chandra, S., Sobczak, W. V., Davydov, S. P., Davydova, A. I., Spektor, V. V., &
 1067 Anthony, K. M. W. (2017). Variable respiration rates of incubated permafrost soil extracts
 1068 from the Kolyma River lowlands, north-east Siberia. *POLAR RESEARCH*, 36.
 1069 <https://doi.org/10.1080/17518369.2017.1305157>
- 1070 Holmes, R. M., McClelland, J. W., Peterson, B. J., Tank, S. E., Bulygina, E., Eglinton, T. I., ...
 1071 Zimov, S. A. (2012). Seasonal and Annual Fluxes of Nutrients and Organic Matter from
 1072 Large Rivers to the Arctic Ocean and Surrounding Seas. *ESTUARIES AND COASTS*, 35(2),
 1073 369–382. <https://doi.org/10.1007/s12237-011-9386-6>
- 1074 Hugelius, G., Strauss, J., Zubrzycki, S., Harden, J. W., Schuur, E. A. G., Ping, C. L., ... Kuhry,
 1075 P. (2014). Estimated stocks of circumpolar permafrost carbon with quantified uncertainty
 1076 ranges and identified data gaps. *Biogeosciences*, 11(23), 6573–6593.
 1077 <https://doi.org/10.5194/bg-11-6573-2014>
- 1078 Hugelius, Gustaf, Loisel, J., Chadburn, S., Jackson, R. B., Jones, M., MacDonald, G., ... Yu, Z.
 1079 (2020). Large stocks of peatland carbon and nitrogen are vulnerable to permafrost thaw.
 1080 *Proceedings of the National Academy of Sciences*, 117(34), 20438–20446.
 1081 <https://doi.org/10.1073/pnas.1916387117>
- 1082 Hultman, J., Waldrop, M. P., Mackelprang, R., David, M. M., McFarland, J., Blazewicz, S. J., ...
 1083 Jansson, J. K. (2015). Multi-omics of permafrost, active layer and thermokarst bog soil
 1084 microbiomes. *Nature*, 521(7551). <https://doi.org/10.1038/nature14238>
- 1085 Jorgenson, M. T., Shur, Y. L., & Pullman, E. R. (2006). Abrupt increase in permafrost
 1086 degradation in Arctic Alaska. *Geophysical Research Letters*, 33(2).
 1087 <https://doi.org/10.1029/2005GL024960>
- 1088 Kalbitz K, Sloinger S, Park JH, Michalzik B, Matzner E (2000) Controls on the dynamics of
 1089 dissolved organic matter in soils: a review. *Soil Science*, 165, 277–304.
- 1090 Kawahigashi, M., Kaiser, K., Rodionov, A., & Guggenberger, G. (2006). Sorption of dissolved
 1091 organic matter by mineral soils of the Siberian forest tundra. *GLOBAL CHANGE*
 1092 *BIOLOGY*, 12(10), 1868–1877. <https://doi.org/10.1111/j.1365-2486.2006.01203.x>
- 1093 Keskitalo, K. H., Bröder, L., Shakil, S., Zolkos, S., Tank, S. E., van Dongen, B. E., ... Vonk, J.
 1094 E. (2021). Downstream Evolution of Particulate Organic Matter Composition From

- 1095 Permafrost Thaw Slumps. *Frontiers in Earth Science*, 9.
1096 <https://doi.org/10.3389/feart.2021.642675>
- 1097 Kicklighter, D. W., Hayes, D. J., McClelland, J. W., Peterson, B. J., McGuire, A. D., & Melillo,
1098 J. M. (2013). Insights and issues with simulating terrestrial DOC loading of Arctic river
1099 networks. *ECOLOGICAL APPLICATIONS*, 23(8), 1817–1836. <https://doi.org/10.1890/11-1100>
1100 1050.1
- 1101 Kokelj, S. V., & Jorgenson, M. T. (2013). Advances in thermokarst research. *Permafrost and
1102 Periglacial Processes*, 24(2), 108–119. <https://doi.org/10.1002/ppp.1779>
- 1103 Lajeunesse, M. J. (2011). On the meta-analysis of response ratios for studies with correlated and
1104 multi-group designs. *Ecology*, 92(11). <https://doi.org/10.1890/11-0423.1>
- 1105 Lajtha, K., Crow, S. E., Yano, Y., Kaushal, S. S., Sulzman, E., Sollins, P., & Spears, J. D. H.
1106 (2005). Detrital controls on soil solution N and dissolved organic matter in soils: A field
1107 experiment. *Biogeochemistry*, 76(2). <https://doi.org/10.1007/s10533-005-5071-9>
- 1108 Lamit, L. J., Romanowicz, K. J., Potvin, L. R., Lennon, J. T., Tringe, S. G., Chimner, R. A., ...
1109 Lilleskov, E. A. (2021). Peatland microbial community responses to plant functional group
1110 and drought are depth-dependent. *Molecular Ecology*, 30(20).
1111 <https://doi.org/10.1111/mec.16125>
- 1112 Langeveld, J., Bouwman, A. F., van Hoek, W. J., Vilmin, L., Beusen, A. H. W., Mogollón, J. M.,
1113 & Middelburg, J. J. (2020). Estimating dissolved carbon concentrations in global soils: a
1114 global database and model. *SN Applied Sciences*, 2(10), 1–21.
1115 <https://doi.org/10.1007/s42452-020-03290-0>
- 1116 Lantuit, H., Overduin, P. P., Couture, N., Wetterich, S., Aré, F., Atkinson, D., Brown, J.,
1117 Cherkashov, G., Drozdov, D., Forbes, D. L., & Graves-Gaylord, A. (2012). The Arctic
1118 coastal dynamics database: A new classification scheme and statistics on Arctic permafrost
1119 coastlines. *Estuaries and Coasts*, 35(2), 383–400. <https://doi.org/10.1007/s12237-010-9362-6>
1120 6
- 1121 Lara, M. J., Nitze, I., Grosse, G., Martin, P., & David McGuire, A. (2018). Reduced arctic tundra
1122 productivity linked with landform and climate change interactions. *Scientific Reports*, 8(1).
1123 <https://doi.org/10.1038/s41598-018-20692-8>
- 1124 Liljedahl, A. K., Boike, J., Daanen, R. P., Fedorov, A. N., Frost, G. V., Grosse, G., ... Zona, D.
1125 (2016). Pan-Arctic ice-wedge degradation in warming permafrost and its influence on
1126 tundra hydrology. *Nature Geoscience*, 9(4). <https://doi.org/10.1038/ngeo2674>
- 1127 Limpens, J., Bohlin, E., & Nilsson, M. B. (2017). Phylogenetic or environmental control on the
1128 elemental and organo-chemical composition of Sphagnum mosses? *Plant and Soil*.
1129 <https://doi.org/10.1007/s11104-017-3239-4>

- 1130 Loiko, S. V, Pokrovsky, O. S., Raudina, T. V, Lim, A., Kolesnichenko, L. G., Shirokova, L. S.,
 1131 ... Kirpotin, S. N. (2017). Abrupt permafrost collapse enhances organic carbon, CO₂,
 1132 nutrient and metal release into surface waters. *Chemical Geology*, 471, 153–165.
 1133 <https://doi.org/https://doi.org/10.1016/j.chemgeo.2017.10.002>
- 1134 Ma, Q., Jin, H., Yu, C., & Bense, V. F. (2019). Dissolved organic carbon in permafrost regions:
 1135 A review. *Science China Earth Sciences*. <https://doi.org/10.1007/s11430-018-9309-6>
- 1136 MacDonald, E. N., Tank, S. E., Kokelj, S. V., Froese, D. G., & Hutchins, R. H. S. (2021).
 1137 Permafrost-derived dissolved organic matter composition varies across permafrost end-
 1138 members in the western Canadian Arctic. *Environmental Research Letters*, 16(2).
 1139 <https://doi.org/10.1088/1748-9326/abd971>
- 1140 Manies, K. L., Jones, M. C., Waldrop, M. P., Leewis, M. C., Fuller, C., Cornman, R. S., &
 1141 Hoefke, K. (2021). Influence of Permafrost Type and Site History on Losses of Permafrost
 1142 Carbon After Thaw. *Journal of Geophysical Research: Biogeosciences*, 126(11).
 1143 <https://doi.org/10.1029/2021JG006396>
- 1144 Marschner B, Bredow A (2002) Temperature effects on release and ecologically relevant
 1145 properties of dissolved organic carbon in sterilised and biologically active soil samples. *Soil*
 1146 *Biology and Biochemistry*, 34, 459–466.
- 1147 McGuire, A. D., Lawrence, D. M., Koven, C., Clein, J. S., Burke, E., Chen, G., ... Zhuang, Q.
 1148 (2018). Dependence of the evolution of carbon dynamics in the northern permafrost region
 1149 on the trajectory of climate change. *Proceedings of the National Academy of Sciences of the*
 1150 *United States of America*, 115(15). <https://doi.org/10.1073/pnas.1719903115>
- 1151 Mehmood, T., Liland, K. H., Snipen, L., & Sæbø, S. (2012). A review of variable selection
 1152 methods in Partial Least Squares Regression. *Chemometrics and Intelligent Laboratory*
 1153 *Systems*. <https://doi.org/10.1016/j.chemolab.2012.07.010>
- 1154 Mevik, B. H., & Wehrens, R. (2007). The pls package: Principal component and partial least
 1155 squares regression in R. *Journal of Statistical Software*, 18(2).
 1156 <https://doi.org/10.18637/jss.v018.i02>
- 1157 Miner, K. R., Turetsky, M. R., Malina, E., Bartsch, A., Tamminen, J., McGuire, A. D., ... Miller,
 1158 C. E. (2022). Permafrost carbon emissions in a changing Arctic. *Nature Reviews Earth and*
 1159 *Environment*. <https://doi.org/10.1038/s43017-021-00230-3>
- 1160 Mohammed, A. A., Guimond, J. A., Bense, V. F., Jamieson, R. C., McKenzie, J. M., & Kurylyk,
 1161 B. L. (2022). Mobilization of subsurface carbon pools driven by permafrost thaw and
 1162 reactivation of groundwater flow: a virtual experiment. *Environmental Research Letters*,
 1163 17(12), 124036. <https://doi.org/10.1088/1748-9326/ACA701>
- 1164 Monteux, S., Weedon, J. T., Blume-Werry, G., Gavazov, K., Jassey, V. E. J., Johansson, M., ...
 1165 Dorrepaal, E. (2018). Long-term in situ permafrost thaw effects on bacterial communities

- 1166 and potential aerobic respiration. *ISME Journal*, 12(9), 2129–2141.
 1167 <https://doi.org/10.1038/s41396-018-0176-z>
- 1168 Moore, T. R., & Dalva, M. (2001). Some controls on the release of dissolved organic carbon by
 1169 plant tissues and soils. *Soil Science*, 166(1), 38–47. [https://doi.org/10.1097/00010694-](https://doi.org/10.1097/00010694-200101000-00007)
 1170 [200101000-00007](https://doi.org/10.1097/00010694-200101000-00007)
- 1171 Neff, J. C., & Hooper, D. U. (2002). Vegetation and climate controls on potential CO₂, DOC and
 1172 DON production in northern latitude soils. *Global Change Biology*, 8(9), 872–884.
 1173 <https://doi.org/10.1046/j.1365-2486.2002.00517.x>
- 1174 O’Donnell, J. A., Aiken, G. R., Butler, K. D., Guillemette, F., Podgorski, D. C., & Spencer, R.
 1175 G. M. (2016). DOM composition and transformation in boreal forest soils: The effects of
 1176 temperature and organic-horizon decomposition state. *Journal of Geophysical Research:*
 1177 *Biogeosciences*, 121(10), 2727–2744. <https://doi.org/10.1002/2016JG003431>.Received
- 1178 Olefeldt, D., Heffernan, L., Jones, M. C., Sannel, A. B. K., Treat, C. C., & Turetsky, M. R.
 1179 (2021). Permafrost Thaw in Northern Peatlands: Rapid Changes in Ecosystem and
 1180 Landscape Functions (pp. 27–67). https://doi.org/10.1007/978-3-030-71330-0_3
- 1181 Olefeldt, D., & Roulet, N. T. (2012). Effects of permafrost and hydrology on the composition
 1182 and transport of dissolved organic carbon in a subarctic peatland complex. *Journal of*
 1183 *Geophysical Research: Biogeosciences*, 117(1). <https://doi.org/10.1029/2011JG001819>
- 1184 Olefeldt, D., & Roulet, N. T. (2014). Permafrost conditions in peatlands regulate magnitude,
 1185 timing, and chemical composition of catchment dissolved organic carbon export. *GLOBAL*
 1186 *CHANGE BIOLOGY*, 20(10), 3122–3136. <https://doi.org/10.1111/gcb.12607>
- 1187 Olefeldt, D., Roulet, N. T., Bergeron, O., Crill, P., Bäckstrand, K., & Christensen, T. R. (2012).
 1188 Net carbon accumulation of a high-latitude permafrost palsa mire similar to permafrost-free
 1189 peatlands. *Geophysical Research Letters*, 39(3). <https://doi.org/10.1029/2011GL050355>
- 1190 Olefeldt, D., Goswami, S., Grosse, G., Hayes, D., Hugelius, G., Kuhry, P., ... Turetsky, M. R.
 1191 (2016). Circumpolar distribution and carbon storage of thermokarst landscapes. *Nature*
 1192 *Communications*, 7, 13043. <https://doi.org/10.1038/ncomms13043>
- 1193 Olson, D. M., Dinerstein, E., Wikramanayake, E. D., Burgess, N. D., Powell, G. V. N.,
 1194 Underwood, E. C., ... others. (2001). Terrestrial Ecoregions of the World: A New Map of
 1195 Life on Earth: A new global map of terrestrial ecoregions provides an innovative tool for
 1196 conserving biodiversity. *BioScience*, 51(11).
- 1197 Panneer Selvam, B., Lapierre, J.-F., Guillemette, F., Voigt, C., Lamprecht, R. E., Biasi, C., ...
 1198 Berggren, M. (2017). Degradation potentials of dissolved organic carbon (DOC) from
 1199 thawed permafrost peat. *SCIENTIFIC REPORTS*, 7, 45811.
 1200 <https://doi.org/10.1038/srep45811>

- 1201 Parmentier, F.J.W., Christensen, T.R., Rysgaard, S. et al. A synthesis of the arctic terrestrial and
 1202 marine carbon cycles under pressure from a dwindling cryosphere. *Ambio* 46 (Suppl 1), 53–
 1203 69 (2017). <https://doi.org/10.1007/s13280-016-0872-8>
- 1204 Payandi-Rolland, D., Shirokova, L. S., Tesfa, M., Bénézeth, P., Lim, A. G., Kuzmina, D., ...
 1205 Pokrovsky, O. S. (2020). Dissolved organic matter biodegradation along a hydrological
 1206 continuum in permafrost peatlands. *Science of The Total Environment*, 749, 141463.
 1207 <https://doi.org/10.1016/J.SCITOTENV.2020.141463>
- 1208 Peacock, M., Fitter, M. N., Jutterström, S., Kothawala, D. N., Moldan, F., Stadmark, J., &
 1209 Evans, C. D. (2022). Three Decades of Changing Nutrient Stoichiometry from Source to
 1210 Sea on the Swedish West Coast. *Ecosystems*, 25(8). <https://doi.org/10.1007/s10021-022-00798-x>
- 1212 Pries, C. E. H., Schuur, E. A. G., & Crummer, K. G. (2012). Holocene Carbon Stocks and
 1213 Carbon Accumulation Rates Altered in Soils Undergoing Permafrost Thaw. *Ecosystems*,
 1214 15(1). <https://doi.org/10.1007/s10021-011-9500-4>
- 1215 Prokushkin, A. S., Gavrilenko, I. V., Abaimov, A. P., Prokushkin, S. G., & Samusenko, A. V.
 1216 (2006). Dissolved organic carbon in upland forested watersheds underlain by continuous
 1217 permafrost in Central Siberia. *Mitigation and Adaptation Strategies for Global Change*,
 1218 11(1), 223–240. <https://doi.org/10.1007/s11027-006-1022-6>
- 1219 Prokushkin, A S, Kajimoto, T., Prokushkin, S. G., McDowell, W. H., Abaimov, A. P., &
 1220 Matsuura, Y. (2005). Climatic factors influencing fluxes of dissolved organic carbon from
 1221 the forest floor in a continuous-permafrost Siberian watershed. *CANADIAN JOURNAL OF*
 1222 *FOREST RESEARCH*, 35(9), 2130–2140. <https://doi.org/10.1139/X05-150>
- 1223 Prokushkin, Anatoly S., Kawahigashi, M., & Tokareva, I. V. (2008). Global Warming and
 1224 Dissolved Organic Carbon Release from Permafrost Soils. In *Permafrost Soils* (pp. 237–
 1225 250). https://doi.org/10.1007/978-3-540-69371-0_16
- 1226 Quinton, W. L., Hayashi, M., & Chasmer, L. E. (2011). Permafrost-thaw-induced land-cover
 1227 change in the Canadian subarctic: Implications for water resources. *Hydrological Processes*,
 1228 25(1), 152–158. <https://doi.org/10.1002/hyp.7894>
- 1229 Quinton, W. L., Hayashi, M., & Pietroniro, A. (2003). Connectivity and storage functions of
 1230 channel fens and flat bogs in northern basins. *Hydrological Processes*.
 1231 <https://doi.org/10.1002/hyp.1369>
- 1232 Rantanen, M., Karpechko, A., Lipponen, A., Nordling, K., Hyvärinen, O., Ruosteenoja, K., ...
 1233 Laaksonen, A. (2021). The Arctic has warmed four times faster than the globe since 1980.
 1234 *Nature Portfolio*, (2022), 0–29. <https://doi.org/https://doi.org/10.1038/s43247-022-00498-3>
- 1235 Raymond, P. A., McClelland, J. W., Holmes, R. M., Zhulidov, A. V., Mull, K., Peterson, B. J.,
 1236 ... Gurtovaya, T. Y. (2007). Flux and age of dissolved organic carbon exported to the Arctic

- 1237 Ocean: A carbon isotopic study of the five largest arctic rivers. *Global Biogeochemical*
1238 *Cycles*, 21(4). <https://doi.org/10.1029/2007GB002934>
- 1239 Ripley, B., Venables, B., Bates, D. M., Hornik, K., Gebhardt, A., & Firth, D. (2019). Package
1240 'MASS' (Version 7.3-51.4). *Cran-R Project*.
- 1241 Schaefer, K., Lantuit, H., Romanovsky, V. E., Schuur, E. A. G., & Witt, R. (2014). The impact
1242 of the permafrost carbon feedback on global climate. *Environmental Research Letters*.
1243 <https://doi.org/10.1088/1748-9326/9/8/085003>
- 1244 Schuur, E. A. G., Abbott, B. W., Commane, R., Ernakovich, J., Euskirchen, E., Hugelius, G.,
1245 Grosse, G., Jones, M., Koven, C., Leshyk, V., Lawrence, D., Lorant, M. M., Mauritz, M.,
1246 Olefeldt, D., Natali, S., Rodenhizer, H., Salmon, V., Schädel, C., Strauss, J., ... Turetsky,
1247 M. (2022). Permafrost and climate change: Carbon cycle feedbacks from the warming
1248 arctic. *Annual Review of Environment and Resources*, 47, 343–371.
- 1249 Schuur, E. A. G., Bracho, R., Celis, G., Belshe, E. F., Ebert, C., Ledman, J., ... Webb, E. E.
1250 (2021). Tundra Underlain By Thawing Permafrost Persistently Emits Carbon to the
1251 Atmosphere Over 15 Years of Measurements. *Journal of Geophysical Research:*
1252 *Biogeosciences*, 126(6), 1–23. <https://doi.org/10.1029/2020jg006044>
- 1253 Schuur, T., McGuire, A. D., Romanovsky, V., Schädel, C., & Mack, M. (2018). Chapter 11:
1254 Arctic and Boreal Carbon. Second State of the Carbon Cycle Report. *Second State of the*
1255 *Carbon Cycle Report (SOCCR2): A Sustained Assessment Report*, 428–468. Retrieved from
1256 <https://carbon2018.globalchange.gov/chapter/11/>
- 1257 Selvam, B. P., Lapierre, J.-F., Guillemette, F., Voigt, C., Lamprecht, R. E., Biasi, C., ...
1258 Berggren, M. (2017). Degradation potentials of dissolved organic carbon (DOC) from
1259 thawed permafrost peat. *SCIENTIFIC REPORTS*, 7. <https://doi.org/10.1038/srep45811>
- 1260 Semenchuk, P. R., Elberling, B., Amtorp, C., Winkler, J., Rumpf, S., Michelsen, A., & Cooper,
1261 E. J. (2015). Deeper snow alters soil nutrient availability and leaf nutrient status in high
1262 Arctic tundra. *Biogeochemistry*, 124(1–3), 81–94. [https://doi.org/10.1007/s10533-015-](https://doi.org/10.1007/s10533-015-0082-7)
1263 [0082-7](https://doi.org/10.1007/s10533-015-0082-7)
- 1264 Shakil, S., Tank, S. E., Kokelj, S. V., Vonk, J. E., & Zolkos, S. (2020). Particulate dominance of
1265 organic carbon mobilization from thaw slumps on the Peel Plateau, NT: Quantification and
1266 implications for stream systems and permafrost carbon release. *Environmental Research*
1267 *Letters*, 15(11). <https://doi.org/10.1088/1748-9326/abac36>
- 1268 Sobek, S., Tranvik, L. J., Prairie, Y. T., Kortelainen, P., & Cole, J. J. (2007). Patterns and
1269 regulation of dissolved organic carbon: An analysis of 7,500 widely distributed lakes.
1270 *Limnology and Oceanography*, 52(3). <https://doi.org/10.4319/lo.2007.52.3.1208>
- 1271 Speetjens, N. J., Tanski, G., Martin, V., Wagner, J., Richter, A., Hugelius, G., ... Vonk, J. E.
1272 (2022). Dissolved organic matter characterization in soils and streams in a small coastal

- 1273 low-arctic catchment. *Biogeosciences*, 19(July), 3073–3097. Retrieved from
1274 <https://doi.org/10.5194/bg-19-3073-2022>
- 1275 Stolpmann, L., Coch, C., Morgenstern, A., Boike, J., Fritz, M., Herzsuh, U., ... Grosse, G.
1276 (2021). First pan-Arctic assessment of dissolved organic carbon in lakes of the permafrost
1277 region. *BIOGEOSCIENCES*, 18(12), 3917–3936. <https://doi.org/10.5194/bg-18-3917-2021>
- 1278 Strauss, J., Laboor, S., Schirrmeister, L., Fedorov, A. N., Fortier, D., Froese, D., ... Grosse, G.
1279 (2021). Circum-Arctic Map of the Yedoma Permafrost Domain. *Frontiers in Earth Science*,
1280 9. <https://doi.org/10.3389/feart.2021.758360>
- 1281 Striegl, R. G., Aiken, G. R., Dornblaser, M. M., Raymond, P. A., & Wickland, K. P. (2005). A
1282 decrease in discharge-normalized DOC export by the Yukon River during summer through
1283 autumn. *GEOPHYSICAL RESEARCH LETTERS*, 32(21).
1284 <https://doi.org/10.1029/2005GL024413>
- 1285 Tank, S. E., Frey, K. E., Striegl, R. G., Raymond, P. A., Holmes, R. M., McClelland, J. W., &
1286 Peterson, B. J. (2012). Landscape-level controls on dissolved carbon flux from diverse
1287 catchments of the circumboreal. *GLOBAL BIOGEOCHEMICAL CYCLES*, 26.
1288 <https://doi.org/10.1029/2012GB004299>
- 1289 Tanski, G., Wagner, D., Knoblauch, C., Fritz, M., Sachs, T., & Lantuit, H. (2019). Rapid CO2
1290 Release From Eroding Permafrost in Seawater. *Geophysical Research Letters*, 46(20).
1291 <https://doi.org/10.1029/2019GL084303>
- 1292 Tanski, George, Bröder, L., Wagner, D., Knoblauch, C., Lantuit, H., Beer, C., ... Vonk, J. E.
1293 (2021). Permafrost Carbon and CO2 Pathways Differ at Contrasting Coastal Erosion Sites
1294 in the Canadian Arctic. *Frontiers in Earth Science*, 9.
1295 <https://doi.org/10.3389/feart.2021.630493>
- 1296 Textor, S. R., Wickland, K. P., Podgorski, D. C., Johnston, S. E., & Spencer, R. G. M. (2019).
1297 Dissolved Organic Carbon Turnover in Permafrost-Influenced Watersheds of Interior
1298 Alaska: Molecular Insights and the Priming Effect. *FRONTIERS IN EARTH SCIENCE*, 7.
1299 <https://doi.org/10.3389/feart.2019.00275>
- 1300 Tfaily, M. M., Hamdan, R., Corbett, J. E., Chanton, J. P., Glaser, P. H., & Cooper, W. T. (2013).
1301 Investigating dissolved organic matter decomposition in northern peatlands using
1302 complimentary analytical techniques. *Geochimica et Cosmochimica Acta*.
1303 <https://doi.org/10.1016/j.gca.2013.03.002>
- 1304 Thurman, E. M. (1985). Organic geochemistry of natural waters (Vol. 2). Springer Science &
1305 Business Media.
- 1306 Treat, C. C., Jones, M. C., Camill, P., Gallego-Sala, A., Garneau, M., Harden, J. W., ...
1307 Välliranta, M. (2016). Effects of permafrost aggradation on peat properties as determined
1308 from a pan-Arctic synthesis of plant macrofossils. *Journal of Geophysical Research:*

- 1309 *Biogeosciences*, 121(1), 78–94. <https://doi.org/10.1002/2015JG003061>
- 1310 Treat, Claire C., & Jones, M. C. (2018). Near-surface permafrost aggradation in Northern
1311 Hemisphere peatlands shows regional and global trends during the past 6000 years.
1312 *Holocene*. <https://doi.org/10.1177/0959683617752858>
- 1313 Turetsky, M. R., Wieder, R. K., Vitt, D. H., Evans, R. J., & Scott, K. D. (2007). The
1314 disappearance of relict permafrost in boreal north America: Effects on peatland carbon
1315 storage and fluxes. *Global Change Biology*, 13(9), 1922–1934.
1316 <https://doi.org/10.1111/j.1365-2486.2007.01381.x>
- 1317 Turetsky, Merritt R., Abbott, B. W., Jones, M. C., Anthony, K. W., Olefeldt, D., Schuur, E. A.
1318 G., ... McGuire, A. D. (2020). Carbon release through abrupt permafrost thaw. *Nature*
1319 *Geoscience*. <https://doi.org/10.1038/s41561-019-0526-0>
- 1320 USDA. (1999). *Soil Taxonomy: A Basic System of Soil Classification for Making and*
1321 *Interpreting Soil Surveys, 2nd Edition. Landscape and Land Capacity.*
- 1322 Varner, R. K., Crill, P. M., Frohling, S., McCalley, C. K., Burke, S. A., Chanton, J. P., ... Palace,
1323 M. W. (2022). Permafrost thaw driven changes in hydrology and vegetation cover increase
1324 trace gas emissions and climate forcing in Stordalen Mire from 1970 to 2014. *Philosophical*
1325 *Transactions of the Royal Society A: Mathematical, Physical and Engineering Sciences*,
1326 380(2215). <https://doi.org/10.1098/rsta.2021.0022>
- 1327 Vonk, J E, Tank, S. E., Mann, P. J., Spencer, R. G. M., Treat, C. C., Striegl, R. G., ... Wickland,
1328 K. P. (2015). Biodegradability of dissolved organic carbon in permafrost soils and aquatic
1329 systems: a meta-analysis. *BIOGEOSCIENCES*, 12(23), 6915–6930.
1330 <https://doi.org/10.5194/bg-12-6915-2015>
- 1331 Vonk, Jorien E., & Gustafsson, Ö. (2013). Permafrost-carbon complexities. *Nature Geoscience*.
1332 <https://doi.org/10.1038/ngeo1937>
- 1333 Vonk, J. E., Mann, P. J., Davydov, S., Davydova, A., Spencer, R. G. M., Schade, J., ... Holmes,
1334 R. M. (2013). High biolability of ancient permafrost carbon upon thaw. *GEOPHYSICAL*
1335 *RESEARCH LETTERS*, 40(11), 2689–2693. <https://doi.org/10.1002/grl.50348>
- 1336 Wang JA, Sulla-Menasha D, Woodcock CE, Sonnentag O, Keeling RF, Friedl MA. Extensive
1337 land cover change across Arctic–Boreal Northwestern North America from disturbance and
1338 climate forcing. *Glob Change Biol*. 2020; 26: 807–822. <https://doi.org/10.1111/gcb.14804>
- 1339 Weishaar, J. L., Aiken, G. R., Bergamaschi, B. A., Fram, M. S., Fujii, R., & Mopper, K. (2003).
1340 Evaluation of specific ultraviolet absorbance as an indicator of the chemical composition
1341 and reactivity of dissolved organic carbon. *Environmental Science and Technology*, 37(20),
1342 4702–4708. <https://doi.org/10.1021/es030360x>
- 1343 Weyhenmeyer, G. A., Fröberg, M., Karlun, E., Khalili, M., Kothawala, D., Temnerud, J., &

1344 Tranvik, L. J. (2012). Selective decay of terrestrial organic carbon during transport from
1345 land to sea. *Global Change Biology*, 18(1). <https://doi.org/10.1111/j.1365->
1346 2486.2011.02544.x

1347 Wickland, K.P., Neff, J. C., & Aiken, G. R. (2007). Dissolved organic carbon in Alaskan boreal
1348 forest: Sources, chemical characteristics, and biodegradability. *Ecosystems*, 10(8), 1323–
1349 1340. <https://doi.org/10.1007/s10021-007-9101-4>

1350 Wickland, Kimberly P, Waldrop, M. P., Aiken, G. R., Koch, J. C., Jorgenson, Mt., & Striegl, R.
1351 G. (2018). Dissolved organic carbon and nitrogen release from boreal Holocene permafrost
1352 and seasonally frozen soils of Alaska. *ENVIRONMENTAL RESEARCH LETTERS*, 13(6).
1353 <https://doi.org/10.1088/1748-9326/aac4ad>

1354 Wild, B., Andersson, A., Broder, L., Vonk, J., Hugelius, G., McClelland, J. W., ... Gustafsson,
1355 O. (2019). Rivers across the Siberian Arctic unearth the patterns of carbon release from
1356 thawing permafrost. *PROCEEDINGS OF THE NATIONAL ACADEMY OF SCIENCES OF*
1357 *THE UNITED STATES OF AMERICA*, 116(21), 10280–10285.
1358 <https://doi.org/10.1073/pnas.1811797116>

1359 Wild, B., Gentsch, N., Capek, P., Diáková, K., Alves, R. J. E., Bárta, J., ... Richter, A. (2016).
1360 Plant-derived compounds stimulate the decomposition of organic matter in arctic permafrost
1361 soils. *Scientific Reports*, 6. <https://doi.org/10.1038/srep25607>

1362 Wild, B., Schnecker, J., Bárta, J., Čapek, P., Guggenberger, G., Hofhansl, F., ... Richter, A.
1363 (2013). Nitrogen dynamics in Turbic Cryosols from Siberia and Greenland. *Soil Biology*
1364 *and Biochemistry*, 67, 85–93. <https://doi.org/https://doi.org/10.1016/j.soilbio.2013.08.004>

1365 Woo, M. (1986). Permafrost hydrology in north america. *Atmosphere - Ocean*, 24(3).
1366 <https://doi.org/10.1080/07055900.1986.9649248>

1367

1368

1369

1370

1371

1372

1373

1374

- 1375
- 1376
- 1377 **Studies used to generate database**
- 1378 Abbott, B. W., Jones, J. B., Godsey, S. E., Larouche, J. R., & Bowden, W. B. (2015). Patterns
1379 and persistence of hydrologic carbon and nutrient export from collapsing upland permafrost.
1380 *Biogeosciences*, 12(12), 3725–3740. <https://doi.org/10.5194/bg-12-3725-2015>
- 1381 Abbott, B. W., Larouche, J. R., Jones, J. J. B., Bowden, W. B., & Balsler, A. W. (2014). From
1382 Thawing and Collapsing Permafrost. *Journal of Geophysical Research: Biogeosciences*,
1383 119, 2049–2063. <https://doi.org/10.1002/2014JG002678>. Received
- 1384 Beckebanze, L., Runkle, B. R. K., Walz, J., Wille, C., Holl, D., Helbig, M., ... Kutzbach, L.
1385 (2022). Lateral carbon export has low impact on the net ecosystem carbon balance of a
1386 polygonal tundra catchment. *BIOGEOSCIENCES*, 19(16), 3863–3876.
1387 <https://doi.org/10.5194/bg-19-3863-2022>
- 1388 Boddy, E., Roberts, P., Hill, P. W., Farrar, J., & Jones, D. L. (2008). Turnover of low molecular
1389 weight dissolved organic C (DOC) and microbial C exhibit different temperature
1390 sensitivities in Arctic tundra soils. *SOIL BIOLOGY & BIOCHEMISTRY*, 40(7), 1557–1566.
1391 <https://doi.org/10.1016/j.soilbio.2008.01.030>
- 1392 Bristol, E. M., Connolly, C. T., Lorenson, T. D., Richmond, B. M., Ilgen, A. G., Choens, R. C.,
1393 ... McClelland, J. W. (2021). Geochemistry of Coastal Permafrost and Erosion-Driven
1394 Organic Matter Fluxes to the Beaufort Sea Near Drew Point, Alaska. *Frontiers in Earth
1395 Science*, 8. <https://doi.org/10.3389/feart.2020.598933>
- 1396 Bruhn, A. D., Stedmon, C. A., Comte, J., Matsuoka, A., Speetjens, N. J., Tanski, G., ... Sjöstedt,
1397 J. (2021). Terrestrial Dissolved Organic Matter Mobilized From Eroding Permafrost
1398 Controls Microbial Community Composition and Growth in Arctic Coastal Zones.
1399 *Frontiers in Earth Science*, 9. <https://doi.org/10.3389/feart.2021.640580>
- 1400 Buckeridge, K. M., & Grogan, P. (2008). Deepened snow alters soil microbial nutrient
1401 limitations in arctic birch hummock tundra. *Applied Soil Ecology*, 39(2), 210–222.
1402 <https://doi.org/https://doi.org/10.1016/j.apsoil.2007.12.010>
- 1403 Burd, K., Estop-Aragonés, C., Tank, S. E., & Olefeldt, D. (2020). Lability of dissolved organic
1404 carbon from boreal peatlands: interactions between permafrost thaw, wildfire, and season.
1405 *Canadian Journal of Soil Science*, 13(February), 1–13. [https://doi.org/10.1139/cjss-2019-
0154](https://doi.org/10.1139/cjss-2019-
1406 0154)
- 1407 Burd, K., Tank, S. E., Dion, N., Quinton, W. L., Spence, C., Tanentzap, A. J., & Olefeldt, D.
1408 (2018). Seasonal shifts in export of DOC and nutrients from burned and unburned peatland-

- 1409 rich catchments, Northwest Territories, Canada. *Hydrology and Earth System Sciences*,
1410 4455–4472. <https://doi.org/10.5194/hess-22-4455-2018>
- 1411 Carey, S. K. (2003). Dissolved organic carbon fluxes in a discontinuous permafrost subarctic
1412 alpine catchment. *PERMAFROST AND PERIGLACIAL PROCESSES*, 14(2), 161–171.
1413 <https://doi.org/10.1002/ppp.444>
- 1414 Chiasson-Poirier, G., Franssen, J., Lafreniere, M. J., Fortier, D., & Lamoureux, S. F. (2020).
1415 Seasonal evolution of active layer thaw depth and hillslope-stream connectivity in a
1416 permafrost watershed. *WATER RESOURCES RESEARCH*, 56(1).
1417 <https://doi.org/10.1029/2019WR025828>
- 1418 Connolly, C. T., Cardenas, M. B., Burkart, G. A., Spencer, R. G. M., & McClelland, J. W.
1419 (2020). Groundwater as a major source of dissolved organic matter to Arctic coastal waters.
1420 *NATURE COMMUNICATIONS*, 11(1). <https://doi.org/10.1038/s41467-020-15250-8>
- 1421 Cory, R. M., Crump, B. C., Dobkowski, J. A., & Kling, G. W. (2013). Surface exposure to
1422 sunlight stimulates CO₂ release from permafrost soil carbon in the Arctic. *Proceedings of*
1423 *the National Academy of Sciences*, 110(9), 3429–3434.
1424 <https://doi.org/10.1073/pnas.1214104110>
- 1425 Deshpande, B. N., Crevecoeur, S., Matveev, A., & Vincent, W. F. (2016). Bacterial production
1426 in subarctic peatland lakes enriched by thawing permafrost. *BIOGEOSCIENCES*, 13(15),
1427 4411–4427. <https://doi.org/10.5194/bg-13-4411-2016>
- 1428 Douglas, T. A., Fortier, D., Shur, Y. L., Kanevskiy, M. Z., Guo, L., Cai, Y., & Bray, M. T.
1429 (2011). Biogeochemical and Geocryological Characteristics of Wedge and Thermokarst-
1430 Cave Ice in the CRREL Permafrost Tunnel, Alaska. *PERMAFROST AND PERIGLACIAL*
1431 *PROCESSES*, 22(2), 120–128. <https://doi.org/10.1002/ppp.709>
- 1432 Drake, T. W., Wickland, K. P., Spencer, R. G. M., McKnight, D. M., & Striegl, R. G. (2015).
1433 Ancient low-molecular-weight organic acids in permafrost fuel rapid carbon dioxide
1434 production upon thaw. *PROCEEDINGS OF THE NATIONAL ACADEMY OF SCIENCES*
1435 *OF THE UNITED STATES OF AMERICA*, 112(45), 13946–13951.
1436 <https://doi.org/10.1073/pnas.1511705112>
- 1437 Dutta, K., Schuur, E. A. G., Neff, J. C., & Zimov, S. A. (2006). Potential carbon release from
1438 permafrost soils of Northeastern Siberia. *GLOBAL CHANGE BIOLOGY*, 12(12), 2336–
1439 2351. <https://doi.org/10.1111/j.1365-2486.2006.01259.x>
- 1440 Edwards, K. A., & Jefferies, R. L. (2013). Inter-annual and seasonal dynamics of soil microbial
1441 biomass and nutrients in wet and dry low-Arctic sedge meadows. *Soil Biology and*
1442 *Biochemistry*, 57, 83–90. <https://doi.org/https://doi.org/10.1016/j.soilbio.2012.07.018>
- 1443 Edwards, K. A., McCulloch, J., Kershaw, G. [Peter, & Jefferies, R. L. (2006). Soil microbial
1444 and nutrient dynamics in a wet Arctic sedge meadow in late winter and early spring. *Soil*

- 1445 *Biology and Biochemistry*, 38(9), 2843–2851.
1446 <https://doi.org/https://doi.org/10.1016/j.soilbio.2006.04.042>
- 1447 Ernakovich, J. G., Lynch, L. M., Brewer, P. E., Calderon, F. J., & Wallenstein, M. D. (2017).
1448 Redox and temperature-sensitive changes in microbial communities and soil chemistry
1449 dictate greenhouse gas loss from thawed permafrost. *BIOGEOCHEMISTRY*, 134(1–2),
1450 183–200. <https://doi.org/10.1007/s10533-017-0354-5>
- 1451 Ewing, S. A., Paces, J. B., O'Donnell, J. A., Jorgenson, M. T., Kanevskiy, M. Z., Aiken, G. R.,
1452 ... Striegl, R. (2015). Uranium isotopes and dissolved organic carbon in loess permafrost:
1453 Modeling the age of ancient ice. *GEOCHIMICA ET COSMOCHIMICA ACTA*, 152, 143–
1454 165. <https://doi.org/10.1016/j.gca.2014.11.008>
- 1455 Fenger-Nielsen, R., Hollesen, J., Matthiesen, H., Andersen, E. A. S., Westergaard-Nielsen, A.,
1456 Harmsen, H., ... Elberling, B. (2019). Footprints from the past: The influence of past human
1457 activities on vegetation and soil across five archaeological sites in Greenland. *Science of the*
1458 *Total Environment*, 654, 895–905. <https://doi.org/10.1016/j.scitotenv.2018.11.018>
- 1459 Fouché, J., Christiansen, C. T., Lafrenière, M. J., Grogan, P., & Lamoureux, S. F. (2020).
1460 Canadian permafrost stores large pools of ammonium and optically distinct
1461 dissolved organic matter. *Nature Communications*, 11(1), 4500.
1462 <https://doi.org/10.1038/s41467-020-18331-w>
- 1463 Fouche, J., Bouchez, C., Keller, C., Allard, M., & Ambrosi, J.-P. (2021). Seasonal cryogenic
1464 processes control supra-permafrost pore water chemistry in two contrasting Cryosols.
1465 *GEODERMA*, 401. <https://doi.org/10.1016/j.geoderma.2021.115302>
- 1466 Fouché, J., Keller, C., Allard, M., Ambrosi, J. P., Fouche, J., Keller, C., ... Ambrosi, J. P. (2014).
1467 Increased CO₂ fluxes under warming tests and soil solution chemistry in Histic and Turbic
1468 Cryosols, Salluit, Nunavik, Canada. *Soil Biology and Biochemistry*, 68, 185–199.
1469 <https://doi.org/https://doi.org/10.1016/j.soilbio.2013.10.007>
- 1470 Fritz, M., Opel, T., Tanski, G., Herzsuh, U., Meyer, H., Eulenburg, A., & Lantuit, H. (2015).
1471 Dissolved organic carbon (DOC) in Arctic ground ice. *CRYOSPHERE*, 9(2), 737–752.
1472 <https://doi.org/10.5194/tc-9-737-2015>
- 1473 Gagné, K. R., Ewers, S. C., Murphy, C. J., Daanen, R., Walter Anthony, K., & Guerard, J. J.
1474 (2020). Composition and photo-reactivity of organic matter from permafrost soils and
1475 surface waters in interior Alaska. *Environmental Science: Processes and Impacts*, 22(7),
1476 1525–1539. <https://doi.org/10.1039/d0em00097c>
- 1477 Gao, L., Zhou, Z., Reyes V, A., & Guo, L. (2018). Yields and Characterization of Dissolved
1478 Organic Matter From Different Aged Soils in Northern Alaska. *JOURNAL OF*
1479 *GEOPHYSICAL RESEARCH-BIOGEOSCIENCES*, 123(7), 2035–2052.
1480 <https://doi.org/10.1029/2018JG004408>

- 1481 Herndon, E. M., Mann, B. F., Chowdhury, T. R., Yang, Z., Wulschleger, S. D., Graham, D., ...
 1482 Gu, B. (2015). Pathways of anaerobic organic matter decomposition in tundra soils from
 1483 Barrow, Alaska. *JOURNAL OF GEOPHYSICAL RESEARCH-BIOGEOSCIENCES*,
 1484 *120*(11), 2345–2359. <https://doi.org/10.1002/2015JG003147>
- 1485 Herndon, E. M., Yang, Z., Bargar, J., Janot, N., Regier, T. Z., Graham, D. E., ... Liang, L.
 1486 (2015). Geochemical drivers of organic matter decomposition in arctic tundra soils.
 1487 *BIOGEOCHEMISTRY*, *126*(3), 397–414. <https://doi.org/10.1007/s10533-015-0165-5>
- 1488 Herndon, E., AlBashaireh, A., Singer, D., Chowdhury, T. [Roy, Gu, B., & Graham, D. (2017).
 1489 Influence of iron redox cycling on organo-mineral associations in Arctic tundra soil.
 1490 *Geochimica et Cosmochimica Acta*, *207*, 210–231.
 1491 <https://doi.org/https://doi.org/10.1016/j.gca.2017.02.034>
- 1492 Heslop, J. K., Chandra, S., Sobczak, W. V., Davydov, S. P., Davydova, A. I., Spektor, V. V., &
 1493 Anthony, K. M. W. (2017). Variable respiration rates of incubated permafrost soil extracts
 1494 from the Kolyma River lowlands, north-east Siberia. *POLAR RESEARCH*, *36*.
 1495 <https://doi.org/10.1080/17518369.2017.1305157>
- 1496 Hirst, C., Mauclet, E., Monhonval, A., Tihon, E., Ledman, J., Schuur, E. A. G., & Opfergelt, S.
 1497 (2022). Seasonal Changes in Hydrology and Permafrost Degradation Control Mineral
 1498 Element-Bound DOC Transport From Permafrost Soils to Streams. *GLOBAL*
 1499 *BIOGEOCHEMICAL CYCLES*, *36*(2). <https://doi.org/10.1029/2021GB007105>
- 1500 Hodgkins, S. B., Tfaily, M. M., Podgorski, D. C., McCalley, C. K., Saleska, S. R., Crill, P. M.,
 1501 ... Cooper, W. T. (2016). Elemental composition and optical properties reveal changes in
 1502 dissolved organic matter along a permafrost thaw chronosequence in a subarctic peatland.
 1503 *Geochimica et Cosmochimica Acta*, *187*, 123–140.
 1504 <https://doi.org/10.1016/j.gca.2016.05.015>
- 1505 Jilkova, V., Devetter, M., Bryndova, M., Hajek, T., Kotas, P., Lulakova, P., ... Macek, P. (2021).
 1506 Carbon Sequestration Related to Soil Physical and Chemical Properties in the High Arctic.
 1507 *GLOBAL BIOGEOCHEMICAL CYCLES*, *35*(9). <https://doi.org/10.1029/2020GB006877>
- 1508 Kane, E. S., Chivers, M. R., Turetsky, M. R., Treat, C. C., Petersen, D. G., Waldrop, M., ...
 1509 McGuire, A. D. (2013). Response of anaerobic carbon cycling to water table manipulation
 1510 in an Alaskan rich fen. *Soil Biology and Biochemistry*, *58*, 50–60.
 1511 <https://doi.org/https://doi.org/10.1016/j.soilbio.2012.10.032>
- 1512 Kane, E. S., Valentine, D. W., Michaelson, G. J., Fox, J. D., & Ping, C.-L. (2006). Controls over
 1513 pathways of carbon efflux from soils along climate and black spruce productivity gradients
 1514 in interior Alaska. *Soil Biology and Biochemistry*, *38*(6), 1438–1450.
 1515 <https://doi.org/https://doi.org/10.1016/j.soilbio.2005.11.004>
- 1516 Kane, E. S., Turetsky, M. R., Harden, J. W., McGuire, A. D., & Waddington, J. M. (2010).
 1517 Seasonal ice and hydrologic controls on dissolved organic carbon and nitrogen

- 1518 concentrations in a boreal-rich fen. *JOURNAL OF GEOPHYSICAL RESEARCH-*
1519 *BIOGEOSCIENCES*, 115. <https://doi.org/10.1029/2010JG001366>
- 1520 Kawahigashi, M., Prokushkin, A., & Sumida, H. (2011). Effect of fire on solute release from
1521 organic horizons under larch forest in Central Siberian permafrost terrain. *Geoderma*,
1522 166(1), 171–180. <https://doi.org/10.1016/j.geoderma.2011.07.027>
- 1523 Koch, J. C., Runkel, R. L., Striegl, R., & McKnight, D. M. (2013). Hydrologic controls on the
1524 transport and cycling of carbon and nitrogen in a boreal catchment underlain by continuous
1525 permafrost. *JOURNAL OF GEOPHYSICAL RESEARCH-BIOGEOSCIENCES*, 118(2),
1526 698–712. <https://doi.org/10.1002/jgrg.20058>
- 1527 Lim, A. G., Loiko, S. V., Kuzmina, D. M., Krickov, I. V., Shirokova, L. S., Kulizhsky, S. P., ...
1528 Pokrovsky, O. S. (2021). Dispersed ground ice of permafrost peatlands: Potential
1529 unaccounted carbon, nutrient and metal sources. *Chemosphere*, 266, 128953.
1530 <https://doi.org/10.1016/j.chemosphere.2020.128953>
- 1531 Lindborg, T., Rydberg, J., Tröjbom, M., Berglund, S., Johansson, E., Löfgren, A., ... Laudon, H.
1532 (2016). Biogeochemical data from terrestrial and aquatic ecosystems in a periglacial
1533 catchment, West Greenland. *Earth System Science Data*, 8(2), 439–459.
1534 <https://doi.org/10.5194/essd-8-439-2016>
- 1535 Littlefair, C. A., & Tank, S. E. (2018). Biodegradability of Thermokarst Carbon in a Till-
1536 Associated, Glacial Margin Landscape: The Case of the Peel Plateau, NWT, Canada.
1537 *JOURNAL OF GEOPHYSICAL RESEARCH-BIOGEOSCIENCES*, 123(10), 3293–3307.
1538 <https://doi.org/10.1029/2018JG004461>
- 1539 Liu, N., Michelsen, A., & Rinnan, R. (2020). Vegetation and soil responses to added carbon and
1540 nutrients remain six years after discontinuation of long-term treatments. *Science of the Total*
1541 *Environment*, 722, 137885. <https://doi.org/10.1016/j.scitotenv.2020.137885>
- 1542 Loiko, S. V., Pokrovsky, O. S., Raudina, T. V., Lim, A., Kolesnichenko, L. G., Shirokova, L. S.,
1543 ... Kirpotin, S. N. (2017). Abrupt permafrost collapse enhances organic carbon, CO₂,
1544 nutrient and metal release into surface waters. *Chemical Geology*, 471, 153–165.
1545 <https://doi.org/10.1016/j.chemgeo.2017.10.002>
- 1546 MacDonald, E. N., Tank, S. E., Kokelj, S. V., Froese, D. G., & Hutchins, R. H. S. (2021).
1547 Permafrost-derived dissolved organic matter composition varies across permafrost end-
1548 members in the western Canadian Arctic. *Environmental Research Letters*, 16(2).
1549 <https://doi.org/10.1088/1748-9326/abd971>
- 1550 Mangal, V., DeGasparro, S., Beresford, D. V., & Guéguen, C. (2020). Linking molecular and
1551 optical properties of dissolved organic matter across a soil-water interface on Akimiski
1552 Island (Nunavut, Canada). *Science of The Total Environment*, 704, 135415.
1553 <https://doi.org/10.1016/j.scitotenv.2019.135415>

- 1554 Masyagina, O. V, Tokareva, I. V, & Prokushkin, A. S. (2016). Post fire organic matter
1555 biodegradation in permafrost soils: Case study after experimental heating of mineral
1556 horizons. *Science of The Total Environment*, 573, 1255–1264.
1557 <https://doi.org/https://doi.org/10.1016/j.scitotenv.2016.04.195>
- 1558 McFarlane, K. J., Throckmorton, H. M., Heikoop, J. M., Newman, B. D., Hedgpeth, A. L.,
1559 Repasch, M. N., ... Wilson, C. J. (2022). Age and chemistry of dissolved organic carbon
1560 reveal enhanced leaching of ancient labile carbon at the permafrost thaw zone.
1561 *BIOGEOSCIENCES*, 19(4), 1211–1223. <https://doi.org/10.5194/bg-19-1211-2022>
- 1562 Mörsdorf, M. A., Baggesen, N. S., Yoccoz, N. G., Michelsen, A., Elberling, B., Ambus, P. L., &
1563 Cooper, E. J. (2019). Deepened winter snow significantly influences the availability and
1564 forms of nitrogen taken up by plants in High Arctic tundra. *Soil Biology and Biochemistry*,
1565 135, 222–234. <https://doi.org/https://doi.org/10.1016/j.soilbio.2019.05.009>
- 1566 Neff, J. C., & Hooper, D. U. (2002). Vegetation and climate controls on potential CO₂, DOC and
1567 DON production in northern latitude soils. *Global Change Biology*, 8(9), 872–884.
1568 <https://doi.org/10.1046/j.1365-2486.2002.00517.x>
- 1569 Nielsen, C. S., Michelsen, A., Strobel, B. W., Wulff, K., Banyasz, I., & Elberling, B. (2017).
1570 Correlations between substrate availability, dissolved CH₄, and CH₄ emissions in an arctic
1571 wetland subject to warming and plant removal. *JOURNAL OF GEOPHYSICAL*
1572 *RESEARCH-BIOGEOSCIENCES*, 122(3), 645–660. <https://doi.org/10.1002/2016JG003511>
- 1573 O'Donnell, J. A., Aiken, G. R., Butler, K. D., Guillemette, F., Podgorski, D. C., & Spencer, R.
1574 G. M. (2016). DOM composition and transformation in boreal forest soils: The effects of
1575 temperature and organic-horizon decomposition state. *JOURNAL OF GEOPHYSICAL*
1576 *RESEARCH-BIOGEOSCIENCES*, 121(10), 2727–2744.
1577 <https://doi.org/10.1002/2016JG003431>
- 1578 O'Donnell, J. A., Turetsky, M. R., Harden, J. W., Manies, K. L., Pruet, L. E., Shetler, G., &
1579 Neff, J. C. (2009). Interactive Effects of Fire, Soil Climate, and Moss on CO₂ Fluxes in
1580 Black Spruce Ecosystems of Interior Alaska. *ECOSYSTEMS*, 12(1), 57–72.
1581 <https://doi.org/10.1007/s10021-008-9206-4>
- 1582 Oiffer, L., & Siciliano, S. D. (2009). Methyl mercury production and loss in Arctic soil. *Science*
1583 *of the Total Environment*, 407(5), 1691–1700.
1584 <https://doi.org/10.1016/j.scitotenv.2008.10.025>
- 1585 Olefeldt, D., & Roulet, N. T. (2012). Effects of permafrost and hydrology on the composition
1586 and transport of dissolved organic carbon in a subarctic peatland complex. *Journal of*
1587 *Geophysical Research: Biogeosciences*, 117(1). <https://doi.org/10.1029/2011JG001819>
- 1588 Olefeldt, D., & Roulet, N. T. (2014). Permafrost conditions in peatlands regulate magnitude,
1589 timing, and chemical composition of catchment dissolved organic carbon export. *Global*
1590 *Change Biology*, 20(10), 3122–3136. <https://doi.org/10.1111/gcb.12607>

- 1591 Olefeldt, D., Roulet, N. T., Bergeron, O., Crill, P., Bäckstrand, K., & Christensen, T. R. (2012).
1592 Net carbon accumulation of a high-latitude permafrost tundra mire similar to permafrost-free
1593 peatlands. *Geophysical Research Letters*. <https://doi.org/10.1029/2011GL050355>
- 1594 Olsrud, M., & Christensen, T. R. (2011). Carbon partitioning in a wet and a semiwet subarctic
1595 mire ecosystem based on in situ ¹⁴C pulse-labelling. *Soil Biology and Biochemistry*, *43*(2),
1596 231–239. <https://doi.org/10.1016/j.soilbio.2010.09.034>
- 1597 Pastor, A., Poblador, S., Skovsholt, L. J., & Riis, T. (2020). Microbial carbon and nitrogen
1598 processes in high-Arctic riparian soils. *PERMAFROST AND PERIGLACIAL PROCESSES*,
1599 *31*(1), 223–236. <https://doi.org/10.1002/ppp.2039>
- 1600 Patzner, M. S., Mueller, C. W., Malusova, M., Baur, M., Nikeleit, V., Scholten, T., ... Bryce, C.
1601 (2020). Iron mineral dissolution releases iron and associated organic carbon during
1602 permafrost thaw. *Nature Communications*, *11*(1), 1–11. <https://doi.org/10.1038/s41467-020-20102-6>
1603
- 1604 Patzner, M. S., Logan, M., McKenna, A. M., Young, R. B., Zhou, Z., Joss, H., ... Bryce, C.
1605 (2022). Microbial iron cycling during tundra hillslope collapse promotes greenhouse gas
1606 emissions before complete permafrost thaw. *Communications Earth & Environment*, *3*(1),
1607 76. <https://doi.org/10.1038/s43247-022-00407-8>
- 1608 Payandi-Rolland, D., Shirokova, L. S., Tesfa, M., Bénézech, P., Lim, A. G., Kuzmina, D., ...
1609 Pokrovsky, O. S. (2020). Dissolved organic matter biodegradation along a hydrological
1610 continuum in permafrost peatlands. *Science of The Total Environment*, *749*, 141463.
1611 <https://doi.org/10.1016/j.scitotenv.2020.141463>
- 1612 Payandi-Rolland, D., Shirokova, L. S., Labonne, F., Bénézech, P., & Pokrovsky, O. S. (2021).
1613 Impact of freeze-thaw cycles on organic carbon and metals in waters of
1614 permafrost peatlands. *Chemosphere*, *279*, 130510.
1615 <https://doi.org/10.1016/j.chemosphere.2021.130510>
- 1616 Payandi-Rolland, D., Shirokova, L. S., Nakhle, P., Tesfa, M., Abdou, A., Causserand, C., ...
1617 Pokrovsky, O. S. (2020). Aerobic release and biodegradation of dissolved organic matter
1618 from frozen peat: Effects of temperature and heterotrophic bacteria. *CHEMICAL*
1619 *GEOLOGY*, *536*. <https://doi.org/10.1016/j.chemgeo.2019.119448>
- 1620 Petersen, D. G., Blazewicz, S. J., Firestone, M., Herman, D. J., Turetsky, M., & Waldrop, M.
1621 (2012). Abundance of microbial genes associated with nitrogen cycling as indices of
1622 biogeochemical process rates across a vegetation gradient in Alaska. *Environmental*
1623 *Microbiology*, *14*(4), 993–1008. <https://doi.org/10.1111/j.1462-2920.2011.02679.x>
- 1624 Pokrovsky, O. S., Reynolds, B. C., Prokushkin, A. S., Schott, J., & Viers, J. (2013). Silicon
1625 isotope variations in Central Siberian rivers during basalt weathering in permafrost-
1626 dominated larch forests. *Chemical Geology*, *355*, 103–116.
1627 <https://doi.org/10.1016/j.chemgeo.2013.07.016>

- 1628 Pokrovsky, O. S., Schott, J., Kudryavtzev, D. I., & Dupré, B. (2005). Basalt weathering in
1629 Central Siberia under permafrost conditions. *Geochimica et Cosmochimica Acta*, 69(24),
1630 5659–5680. <https://doi.org/10.1016/j.gca.2005.07.018>
- 1631 Pokrovsky, O. S., Manasypov, R. M., Loiko, S. V., & Shirokova, L. S. (2016). Organic and
1632 organo-mineral colloids in discontinuous permafrost zone. *Geochimica et Cosmochimica*
1633 *Acta*, 188, 1–20. <https://doi.org/10.1016/j.gca.2016.05.035>
- 1634 Poulin, B. A., Ryan, J. N., Tate, M. T., Krabbenhoft, D. P., Hines, M. E., Barkay, T., ... Aiken,
1635 G. R. (2019). Geochemical Factors Controlling Dissolved Elemental Mercury and
1636 Methylmercury Formation in Alaskan Wetlands of Varying Trophic Status. *Environmental*
1637 *Science and Technology*, 53(11), 6203–6213. <https://doi.org/10.1021/acs.est.8b06041>
- 1638 Prokushkin, A. S., Gavrilenko, I. V., Abaimov, A. P., Prokushkin, S. G., & Samusenko, A. V.
1639 (2006). Dissolved organic carbon in upland forested watersheds underlain by continuous
1640 permafrost in Central Siberia. *Mitigation and Adaptation Strategies for Global Change*,
1641 11(1), 223–240. <https://doi.org/10.1007/s11027-006-1022-6>
- 1642 Prokushkin, A. S., Gleixner, G., McDowell, W. H., Ruehlow, S., & Schulze, E.-D. (2007).
1643 Source- and substrate-specific export of dissolved organic matter from permafrost-
1644 dominated forested watershed in central Siberia. *GLOBAL BIOGEOCHEMICAL CYCLES*,
1645 21(4). <https://doi.org/10.1029/2007GB002938>
- 1646 Prokushkin, A. S., Kajimoto, T., Prokushkin, S. G., McDowell, W. H., Abaimov, A. P., &
1647 Matsuura, Y. (2005). Climatic factors influencing fluxes of dissolved organic carbon from
1648 the forest floor in a continuous-permafrost Siberian watershed. *CANADIAN JOURNAL OF*
1649 *FOREST RESEARCH*, 35(9), 2130–2140. <https://doi.org/10.1139/X05-150>
- 1650 Rasmussen, L. H., Michelsen, A., Ladegaard-Pedersen, P., Nielsen, C. S., & Elberling, B.
1651 (2020). Arctic soil water chemistry in dry and wet tundra subject to snow addition, summer
1652 warming and herbivory simulation. *Soil Biology and Biochemistry*, 141, 107676.
1653 <https://doi.org/10.1016/j.soilbio.2019.107676>
- 1654 Raudina, T. V., Loiko, S. V., Lim, A., Manasypov, R. M., Shirokova, L. S., Istigechev, G. I., ...
1655 Pokrovsky, O. S. (2018). Permafrost thaw and climate warming may decrease the CO₂,
1656 carbon, and metal concentration in peat soil waters of the Western Siberia Lowland. *Science*
1657 *of The Total Environment*, 634, 1004–1023.
1658 <https://doi.org/10.1016/j.scitotenv.2018.04.059>
- 1659 Raudina, T. V., Loiko, S. V., Lim, A. G., Krickov, I. V., Shirokova, L. S., Istigechev, G. I., ...
1660 Pokrovsky, O. S. (2017). Dissolved organic carbon and major and trace elements in peat
1661 porewater of sporadic, discontinuous, and continuous permafrost zones of western Siberia.
1662 *BIOGEOSCIENCES*, 14(14), 3561–3584. <https://doi.org/10.5194/bg-14-3561-2017>

- 1663 Ro, H.-M., Ji, Y., & Lee, B. (2018). Interactive effect of soil moisture and temperature regimes
 1664 on the dynamics of soil organic carbon decomposition in a subarctic tundra soil.
 1665 *GEOSCIENCES JOURNAL*, 22(1), 121–130. <https://doi.org/10.1007/s12303-017-0052-2>
- 1666 Roehm, C. L., Giesler, R., & Karlsson, J. (2009). Bioavailability of terrestrial organic carbon to
 1667 lake bacteria: The case of a degrading subarctic permafrost mire complex. *JOURNAL OF*
 1668 *GEOPHYSICAL RESEARCH-BIOGEOSCIENCES*, 114.
 1669 <https://doi.org/10.1029/2008JG000863>
- 1670 Rogers, J. A., Galy, V., Kellerman, A. M., Chanton, J. P., Zimov, N., & Spencer, R. G. M.
 1671 (2021). Limited Presence of Permafrost Dissolved Organic Matter in the Kolyma River,
 1672 Siberia Revealed by Ramped Oxidation. *JOURNAL OF GEOPHYSICAL RESEARCH-*
 1673 *BIOGEOSCIENCES*, 126(7). <https://doi.org/10.1029/2020JG005977>
- 1674 Roth, V.-N., Dittmar, T., Gaupp, R., & Gleixner, G. (2013). Latitude and pH driven trends in the
 1675 molecular composition of DOM across a north south transect along the Yenisei River.
 1676 *Geochimica et Cosmochimica Acta*, 123, 93–105.
 1677 <https://doi.org/https://doi.org/10.1016/j.gca.2013.09.002>
- 1678 Schostag, M., Stibal, M., Jacobsen, C. S., Baelum, J., Tas, N., Elberling, B., ... Prieme, A.
 1679 (2015). Distinct summer and winter bacterial communities in the active layer of Svalbard
 1680 permafrost revealed by DNA- and RNA-based analyses. *FRONTIERS IN*
 1681 *MICROBIOLOGY*, 6. <https://doi.org/10.3389/fmicb.2015.00399>
- 1682 Shakil, S., Tank, S. E., Kokelj, S. V., Vonk, J. E., & Zolkos, S. (2020). Particulate dominance of
 1683 organic carbon mobilization from thaw slumps on the Peel Plateau, NT: Quantification and
 1684 implications for stream systems and permafrost carbon release. *Environmental Research*
 1685 *Letters*, 15(11). <https://doi.org/10.1088/1748-9326/abac36>
- 1686 Shatilla, N. J., & Carey, S. K. (2019). Assessing inter-annual and seasonal patterns of DOC and
 1687 DOM quality across a complex alpine watershed underlain by discontinuous permafrost in
 1688 Yukon, Canada. *Hydrology and Earth System Sciences*, 23(9), 3571–3591.
 1689 <https://doi.org/10.5194/hess-23-3571-2019>
- 1690 Shirokova, L. S., Pokrovsky, O. S., Kirpotin, S. N., Desmukh, C., Pokrovsky, B. G., Audry, S.,
 1691 & Viers, J. (2013). Biogeochemistry of organic carbon, CO₂, CH₄, and trace elements in
 1692 thermokarst water bodies in discontinuous permafrost zones of Western Siberia.
 1693 *BIOGEOCHEMISTRY*, 113(1–3), 573–593. <https://doi.org/10.1007/s10533-012-9790-4>
- 1694 Shirokova, L. S., Bredoire, R., Rols, J.-L. L., & Pokrovsky, O. S. (2017). Moss and Peat
 1695 Leachate Degradability by Heterotrophic Bacteria: The Fate of Organic Carbon and Trace
 1696 Metals. *Geomicrobiology Journal*, 34(8), 641–655.
 1697 <https://doi.org/10.1080/01490451.2015.1111470>
- 1698 Shirokova, L. S., Chupakov, A. V., Zabelina, S. A., Neverova, N. V., Payandi-Rolland, D.,
 1699 Causserand, C., ... Pokrovsky, O. S. (2019). Humic surface waters of frozen peat bogs

- 1700 (permafrost zone) are highly resistant to bio- and photodegradation. *BIOGEOSCIENCES*,
 1701 16(12), 2511–2526. <https://doi.org/10.5194/bg-16-2511-2019>
- 1702 Shirokova, L. S., Labouret, J., Gurge, M., Gerard, E., Ivanova, I. S., Zabelina, S. A., &
 1703 Pokrovsky, O. S. (2017). Impact of Cyanobacterial Associate and Heterotrophic Bacteria on
 1704 Dissolved Organic Carbon and Metal in Moss and Peat Leachate: Application to Permafrost
 1705 Thaw in Aquatic Environments. *AQUATIC GEOCHEMISTRY*, 23(5–6), 331–358.
 1706 <https://doi.org/10.1007/s10498-017-9325-7>
- 1707 Sistla, S. A., Schaeffer, S., & Schimel, J. P. (2019). Plant community regulates decomposer
 1708 response to freezing more strongly than the rate or extent of the freezing regime.
 1709 *ECOSPHERE*, 10(2). <https://doi.org/10.1002/ecs2.2608>
- 1710 Speetjens, N. J., Tanski, G., Martin, V., Wagner, J., Richter, A., Hugelius, G., ... Vonk, J. E.
 1711 (2022). Dissolved organic matter characterization in soils and streams in a small coastal
 1712 low-arctic catchment. *Biogeosciences*, 19(July), 3073–3097. Retrieved from
 1713 <https://doi.org/10.5194/bg-19-3073-2022>
- 1714 Stutter, M. I., & Billett, M. F. (2003). Biogeochemical controls on streamwater and soil solution
 1715 chemistry in a High Arctic environment. *Geoderma*, 113(1), 127–146.
 1716 [https://doi.org/https://doi.org/10.1016/S0016-7061\(02\)00335-X](https://doi.org/https://doi.org/10.1016/S0016-7061(02)00335-X)
- 1717 Takano, S., Yamashita, Y., Tei, S., Liang, M., Shingubara, R., Morozumi, T., ... Sugimoto, A.
 1718 (2021). Stable Water Isotope Assessment of Tundra Wetland Hydrology as a Potential
 1719 Source of Arctic Riverine Dissolved Organic Carbon in the Indigirka River Lowland,
 1720 Northeastern Siberia. *Frontiers in Earth Science*, 9.
 1721 <https://doi.org/10.3389/feart.2021.699365>
- 1722 Tanski, G., Couture, N., Lantuit, H., Eulenburg, A., & Fritz, M. (2016). Eroding permafrost
 1723 coasts release low amounts of dissolved organic carbon (DOC) from ground ice into the
 1724 nearshore zone of the Arctic Ocean. *Global Biogeochemical Cycles*, 30(7), 1054–1068.
 1725 <https://doi.org/10.1002/2015GB005337>
- 1726 Tanski, G., Lantuit, H., Ruttor, S., Knoblauch, C., Radosavljevic, B., Strauss, J., ... Fritz, M.
 1727 (2017). Transformation of terrestrial organic matter along thermokarst-affected permafrost
 1728 coasts in the Arctic. *Science of the Total Environment*, 581–582, 434–447.
 1729 <https://doi.org/10.1016/j.scitotenv.2016.12.152>
- 1730 Textor, S. R., Wickland, K. P., Podgorski, D. C., Johnston, S. E., & Spencer, R. G. M. (2019).
 1731 Dissolved Organic Carbon Turnover in Permafrost-Influenced Watersheds of Interior
 1732 Alaska: Molecular Insights and the Priming Effect. *FRONTIERS IN EARTH SCIENCE*, 7.
 1733 <https://doi.org/10.3389/feart.2019.00275>
- 1734 Thompson, M. S., Giesler, R., Karlsson, J., & Klaminder, J. (2015). Size and characteristics of
 1735 the DOC pool in near-surface subarctic mire permafrost as a potential source for nearby

- 1736 freshwaters. *Arctic, Antarctic, and Alpine Research*, 47(1), 49–58.
 1737 <https://doi.org/10.1657/AAAR0014-010>
- 1738 Treat, C. C., Wollheim, W. M., Varner, R. K., & Bowden, W. B. (2016). Longer thaw seasons
 1739 increase nitrogen availability for leaching during fall in tundra soils. *ENVIRONMENTAL*
 1740 *RESEARCH LETTERS*, 11(6). <https://doi.org/10.1088/1748-9326/11/6/064013>
- 1741 Trusiak, A., Treibergs, L. A., Kling, G. W., & Cory, R. M. (2018). The role of iron and reactive
 1742 oxygen species in the production of CO₂ in arctic soil waters. *GEOCHIMICA ET*
 1743 *COSMOCHIMICA ACTA*, 224, 80–95. <https://doi.org/10.1016/j.gca.2017.12.022>
- 1744 Voigt, C., Lamprecht, R. E., Marushchak, M. E., Lind, S. E., Novakovskiy, A., Aurela, M., ...
 1745 Biasi, C. (2017). Warming of subarctic tundra increases emissions of all three important
 1746 greenhouse gases – carbon dioxide, methane, and nitrous oxide. *Global Change Biology*,
 1747 23(8), 3121–3138. <https://doi.org/10.1111/gcb.13563>
- 1748 Voigt, C., Marushchak, M. E., Mastepanov, M., Lamprecht, R. E., Christensen, T. R.,
 1749 Dorodnikov, M., ... Biasi, C. (2019). Ecosystem carbon response of an Arctic peatland to
 1750 simulated permafrost thaw. *Global Change Biology*, 25(5), 1746–1764.
 1751 <https://doi.org/10.1111/gcb.14574>
- 1752 Voigt, C., Marushchak, M. E., Lamprecht, R. E., Jackowicz-Korczyński, M., Lindgren, A.,
 1753 Mastepanov, M., ... Biasi, C. (2017). Increased nitrous oxide emissions from Arctic
 1754 peatlands after permafrost thaw. *Proceedings of the National Academy of Sciences of the*
 1755 *United States of America*, 114(24), 6238–6243. Retrieved from
 1756 <https://www.jstor.org/stable/26484198>
- 1757 Vonk, J. E., Mann, P. J., Dowdy, K. L., Davydova, A., Davydov, S. P., Zimov, N., ... Holmes,
 1758 R. M. (2013). Dissolved organic carbon loss from Yedoma permafrost amplified by ice
 1759 wedge thaw. *ENVIRONMENTAL RESEARCH LETTERS*, 8(3).
 1760 <https://doi.org/10.1088/1748-9326/8/3/035023>
- 1761 Vonk, J. E., Mann, P. J., Davydov, S., Davydova, A., Spencer, R. G. M., Schade, J., ... Holmes,
 1762 R. M. (2013). High biolability of ancient permafrost carbon upon thaw. *GEOPHYSICAL*
 1763 *RESEARCH LETTERS*, 40(11), 2689–2693. <https://doi.org/10.1002/grl.50348>
- 1764 Waldrop, M. P., Harden, J. W., Turetsky, M. R., Petersen, D. G., McGuire, A. D., Briones, M. J.
 1765 I., ... Pruet, L. E. (2012). Bacterial and enchytraeid abundance accelerate soil carbon
 1766 turnover along a lowland vegetation gradient in interior Alaska. *Soil Biology and*
 1767 *Biochemistry*, 50, 188–198. <https://doi.org/https://doi.org/10.1016/j.soilbio.2012.02.032>
- 1768 Waldrop, M. P., & Harden, J. W. (2008). Interactive effects of wildfire and permafrost on
 1769 microbial communities and soil processes in an Alaskan black spruce forest. *GLOBAL*
 1770 *CHANGE BIOLOGY*, 14(11), 2591–2602. [https://doi.org/10.1111/j.1365-](https://doi.org/10.1111/j.1365-2486.2008.01661.x)
 1771 [2486.2008.01661.x](https://doi.org/10.1111/j.1365-2486.2008.01661.x)

- 1772 Ward, C. P., & Cory, R. M. (2015). Chemical composition of dissolved organic matter draining
1773 permafrost soils. *Geochimica et Cosmochimica Acta*, *167*, 63–79.
1774 <https://doi.org/https://doi.org/10.1016/j.gca.2015.07.001>
- 1775 Ward, C. P., Nalven, S. G., Crump, B. C., Kling, G. W., & Cory, R. M. (2017). Photochemical
1776 alteration of organic carbon draining permafrost soils shifts microbial metabolic pathways
1777 and stimulates respiration. *NATURE COMMUNICATIONS*, *8*.
1778 <https://doi.org/10.1038/s41467-017-00759-2>
- 1779 Whittinghill, K. A., Finlay, J. C., & Hobbie, S. E. (2014). Bioavailability of dissolved organic
1780 carbon across a hillslope chronosequence in the Kuparuk River region, Alaska. *Soil Biology
1781 and Biochemistry*, *79*, 25–33. <https://doi.org/https://doi.org/10.1016/j.soilbio.2014.08.020>
- 1782 Wickland, K. P., Neff, J. C., & Aiken, G. R. (2007). Dissolved organic carbon in Alaskan boreal
1783 forest: Sources, chemical characteristics, and biodegradability. *ECOSYSTEMS*, *10*(8),
1784 1323–1340. <https://doi.org/10.1007/s10021-007-9101-4>
- 1785 Wickland, K. P., Waldrop, M. P., Aiken, G. R., Koch, J. C., Jorgenson, Mt., & Striegl, R. G.
1786 (2018). Dissolved organic carbon and nitrogen release from boreal Holocene permafrost and
1787 seasonally frozen soils of Alaska. *ENVIRONMENTAL RESEARCH LETTERS*, *13*(6).
1788 <https://doi.org/10.1088/1748-9326/aac4ad>
- 1789 Yun, J., Jung, J. Y., Kwon, M. J., Seo, J., Nam, S., Lee, Y. K., & Kang, H. (2022). Temporal
1790 Variations Rather than Long-Term Warming Control Extracellular Enzyme Activities and
1791 Microbial Community Structures in the High Arctic Soil. *MICROBIAL ECOLOGY*, *84*(1),
1792 168–181. <https://doi.org/10.1007/s00248-021-01859-9>
- 1793 Zolkos, S., & Tank, S. E. (2019). *Permafrost geochemistry and retrogressive thaw slump
1794 morphology (Peel Plateau, Canada)*, v. 1.0 (2017-2017). [https://doi.org/10.5885/45573XD-
1795 28DD57D553F14BF0](https://doi.org/10.5885/45573XD-28DD57D553F14BF0)
- 1796